Western blot analysis

Subconfluent keratinocytes were stimulated with 30 μg/ml hBDs for the indicated time periods. After stimulation, the lysates were obtained by lysing cells in lysis buffer (50 mM Tris-HCl (pH 8), 150 mM NaCl, 0.02% NaN_3, 0.1% SDS, 1% Nonidet P-40, containing 1 μM phenylmethylsulphonyl fluoride, 10 μg/ml leupeptin, 10 μg/ml pepstatin-A, 50 μg/ml aprotinin and 2 mM sodium orthovanadate). The equal amounts of total protein were subjected to 15% SDS-PAGE. After, nonspecific binding sites were blocked, and the blots were incubated with polyclonal antibodies against phosphorylated EGFR, STAT1, and STAT3 or total EGFR, STAT1, and STAT3 overnight, according to the manufacturer's instructions. The membrane was developed with an enhanced chemiluminescence detection kit (Amersham Pharmacia Biotech, Piscataway, NJ). To quantify the intensity of bands, densitometry using the software program Image Gauge (LAS-1000plus, Fujifilm, Tokyo, Japan) was performed to allow correction for protein loading.

Statistical analysis

Statistical analysis was performed using Student's *t*-test or one-way analysis of variance, and $P<0.05$ was considered to be significant. The results are shown as mean ± standard deviation (SD).

All the above studies have Juntendo University institutional approval and adherence to the Declaration of Helsinki Principles.

CONFLICT OF INTEREST

The authors declare no conflict of interest.

ACKNOWLEDGMENTS

We thank Dr Takeshi Kato for his insightful technical assistance and discussion, members of Atopy (Allergy) Research Center and Department of Immunology of Juntendo University School of Medicine for their comments and encouragement, and Michiyo Matsumoto for secretarial assistance. This work was supported in part by Grant-in-Aid for Scientific Research from the Ministry of Education, Culture, Sports, Science, and Technology, Japan to Niyonsaba F., and Atopy (Allergy) Research Center, Juntendo University, Tokyo, Japan.

REFERENCES

Aarbiou J, Ertmann M, van Wetering S, van Noort P, Rook D, Rabe KF *et al.* (2002) Human neutrophil defensins induce lung epithelial cell proliferation *in vitro*. *J Leukoc Biol* 72:167–74

Aarbiou J, Verhoosel RM, van Wetering S, De Boer WI, van Krieken JH, Litvinov SV *et al.* (2004) Neutrophil defensins enhance lung epithelial wound closure and mucin gene expression *in vitro*. *Am J Respir Cell Mol Biol* 30:193–201

Ali RS, Falconer A, Ikram M, Bissett CE, Cerio R, Quinn AG (2001) Expression of the peptide antibiotics human β-defensin-1 and human β-defensin-2 in normal human skin. *J Invest Dermatol* 117:106–11

Andl CD, Mizushima T, Oyama K, Bowser M, Nakagawa H, Rustgi AK (2004) EGFR-induced cell migration is mediated predominantly by the JAK-STAT pathway in primary esophageal keratinocytes. *Am J Physiol Gastrointest Liver Physiol* 287:G1227–37

Befus AD, Mowat C, Gilchrist M, Hu J, Solomon S, Bateman A (1999) Neutrophil defensins induce histamine secretion from mast cells: mechanisms of action. *J Immunol* 163:947–53

Cha D, O'Brien P, O'Toole EA, Woodley DT, Hudson LG (1996) Enhanced modulation of keratinocyte motility by transforming growth factor-α (TGF-α) relative to epidermal growth factor (EGF). *J Invest Dermatol* 106:590–7

Chaly YV, Paleolog EM, Kolesnikova TS, Tikhonov II, Petratchenko EV, Voitenok NN (2000) Neutrophil α-defensin human neutrophil peptide modulates cytokine production in human monocytes and adhesion molecule expression in endothelial cells. *Eur Cytokine Netw* 11:257–66

Chen X, Niyonsaba F, Ushio H, Okuda D, Nagaoka I, Okumura K *et al.* (2005) Synergistic effect of antibacterial agents human β-defensins, cathelicidin LL-37 and lysozyme against *Staphylococcus aureus* and *Escherichia coli*. *J Dermatol Sci* 40:123–32

Chertov O, Michiel DF, Xu L, Wang JM, Tani K, Murphy WJ *et al.* (1996) Identification of defensin-1, defensin-2, and CAP37/azurocidin as T-cell chemoattractant proteins released from interleukin-8-stimulated neutrophils. *J Biol Chem* 271:2935–40

Clapham DE (1995) Calcium signaling. *Cell* 80:259–68

Dorschner RA, Pestonjamasp VK, Tamakuwala S, Ohtake T, Rudisill J, Nizet V *et al.* (2001) Cutaneous injury induces the release of cathelicidin antimicrobial peptides active against group A *Streptococcus*. *J Invest Dermatol* 117:91–7

Frank DA, Mahajan S, Ritz J (1999) Fludarabine-induced immunosuppression is associated with inhibition of STAT1 signaling. *Nat Med* 5:444–7

Frohm NM, Sandstedt B, Sørensen O, Weber G, Borregaard N, Ståhle-Bäckdahl M (1999) The human cationic antimicrobial protein (hCAP-18), a peptide antibiotic, is widely expressed in human squamous epithelia and colocalizes with interleukin-6. *Infect Immun* 67:2561–6

Fulton C, Anderson GM, Zasloff M, Bull R, Quinn AG (1997) Expression of natural peptide antibiotics in human skin. *Lancet* 350:1750–1

García JR, Jaumann F, Schulz S, Krause A, Rodríguez-Jiménez J, Forssmann U *et al.* (2001a) Identification of a novel, multifunctional β-defensin (human β-defensin-3) with specific antimicrobial activity: Its interaction with plasma membranes of *Xenopus* oocytes and the induction of macrophage chemoattraction. *Cell Tissue Res* 306:257–64

García JR, Krause A, Schulz S, Rodríguez-Jiménez FJ., Klüver E, Adermann K *et al.* (2001b) Human β-defensin 4: a novel inducible peptide with a specific salt-sensitive spectrum of antimicrobial activity. *FASEB J* 15:1819–21

Harder J, Bartels J, Christophers E, Schröder JM (1997) A peptide antibiotic from human skin. *Nature* 387:861–2

Harder J, Bartels J, Christophers E, Schröder JM (2001) Isolation and characterization of human β-defensin-3, a novel human inducible peptide antibiotic. *J Biol Chem* 276:5707–13

Harder J, Meyer-Hoffert U, Wehkamp K, Schwichtenberg L, Schröder JM (2004) Differential gene induction of human β-defensins (hBD-1, -2, -3, and -4) in keratinocytes is inhibited by retinoic acid. *J Invest Dermatol* 123:522–9

Heilborn JD, Nilsson MF, Kratz G, Weber G, Sørensen O, Borregaard N *et al.* (2003) The cathelicidin anti-microbial peptide LL-37 is involved in re-epithelialization of human skin wounds and is lacking in chronic ulcer epithelium. *J Invest Dermatol* 120:379–89

Hou C, Kirchner T, Singer M, Matheis M, Argentieri D, Cavender D (2004) *In vivo* activity of a phospholipase C inhibitor, 1-(6-((17beta-3-methoxyestra-1,3,5(10)-trien-17-yl) amino) hexyl)-1H-pyrrole-2,5-dione (U73122), in acute and chronic inflammatory reactions. *J Pharmacol Exp Ther* 309:697–704

Huh WK, Oono T, Shirafuji Y, Akiyama H, Arata J, Sakaguchi M *et al.* (2002) Dynamic alteration of human β-defensin 2 localization from cytoplasm to intercellular space in psoriatic skin. *J Mol Med* 80:678–84

Jia HP, Schutte BC, Schudy A, Linzmeier R, Guthmiller JM, Johnson GK *et al.* (2001) Discovery of new human β-defensins using a genomics-based approach. *Gene* 263:211–8

Kehrl JH (1998) Heterotrimeric G protein signaling: roles in immune function and fine-tuning by RGS proteins. *Immunity* 8:1–10

Kijima T, Niwa H, Steinman RA, Drenning SD, Gooding WE, Wentzel AL *et al.* (2002) STAT3 activation abrogates growth factor dependence and contributes to head and neck squamous cell carcinoma tumor growth *in vivo*. *Cell Growth Differ* 13:355–62

Knall C, Johnson GL (1998) G-protein regulatory pathways: rocketing into the twenty-first century. *J Cell Biochem Suppl* 30/31:137–46

Koczulla R, von Degenfeld G, Kupatt C, Krotz F, Zahler S, Gloe T *et al.* (2003) An angiogenic role for the human peptide antibiotic LL-37/hCAP-18. *J Clin Invest* 111:1665–72

Lehrer IR, Ganz T (1999) Antimicrobial peptides in mammalian and insect host defense. *Curr Opin Immunol* 11:23–7

Li W, Henry G, Fan J, Bandyopadhyay B, Pang K, Garner W *et al.* (2004) Signals that initiate, augment, and provide directionality for human keratinocyte motility. *J Invest Dermatol* 123:622–33

Liu AY, Destoumieux D, Wong AV, Park CH, Valore EV, Liu L *et al.* (2002) Human β-defensin-2 production in keratinocytes is regulated by interleukin-1, bacteria, and the state of differentation. *J Invest Dermatol* 118:275–81

Niyonsaba F, Someya A, Hirata M, Ogawa H, Nagaoka I (2001) Evaluation of the effects of peptide antibiotics human β-defensins-1/-2 and LL-37 on histamine release and prostaglandin D_2 production from mast cells. *Eur J Immunol* 31:1066–75

Niyonsaba F, Iwabuchi K, Matsuda H, Ogawa H, Nagaoka I (2002a) Epithelial cell-derived human β-defensin-2 acts as chemotaxin for mast cells through a pertussis toxin-sensitive and phospholipase C-dependent pathway. *Int Immunol* 14:421–6

Niyonsaba F, Iwabuchi K, Someya A, Hirata M, Matsuda H, Ogawa H *et al.* (2002b) A cathelicidin family of human antibacterial peptide LL-37 induces mast cell chemotaxis. *Immunology* 106:20–6

Niyonsaba F, Ogawa H, Nagaoka I (2004) Human β-defensin-2 functions as a chemotactic agent for tumour necrosis factor-α-treated human neutrophils. *Immunology* 111:273–81

Niyonsaba F, Ushio H, Nagaoka I, Okumura K, Ogawa H (2005) The human β-defensins (hBD-1, -2, -3, -4) and cathelicidin LL-37 induce interleukin-18 secretion through p38 and ERK MAPK activation in primary human keratinocytes. *J Immunol* 175:1776–84

Ong PY, Ohtake T, Btandt C, Strickland L, Boguniewics M, Ganz T *et al.* (2002) Endogenous antimicrobial peptides and skin infections in atopic dermatitis. *New Engl J Med* 347:1151–60

Oppenheim JJ, Biragyn A, Kwak LW, Yang D (2003) Roles of antimicrobial peptides such as defensins in innate and adaptive immunity. *Ann Rheum Dis* 62:17–21

Oren A, Ganz T, Liu L, Meerloo T (2003) In human epidermis, β-defensin 2 is packaged in lamellar bodies. *Exp Mol Pathol* 74:180–2

Sano S, Itami S, Takeda K, Tarutani M, Yamaguchi Y, Miura H *et al.* (1999) Keratinocyte-specific ablation of Stat3 exhibits impaired skin remodeling, but does not affect skin morphogenesis. *EMBO J* 18:4657–68

Shaykhiev R, Bei C, Kändler K, Senske J, Püchner A, Damm T *et al.* (2005) The human endogenous antibiotic LL-37 stimulates airway epithelial cell proliferation and wound closure. *Am J Physiol Lung Cell Mol Physiol* 289:L842–8

Sørensen O, Arnljots K, Cowland JB, Bainton DF, Borregaard N (1997) The human antibacterial cathelicidin, hCAP-18, is synthesized in myelocytes and metamyelocytes and localized to specific granules in neutrophils. *Blood* 90:2796–803

Sørensen OE, Thapa DR, Rosenthal A, Liu L, Roberts AA, Ganz T (2005) Differential regulation of β-defensin expression in human skin by microbial stimuli. *J Immunol* 174:4870–9

Tokumaru S, Sayama K, Shirakata Y, Komatsuzawa H, Ouhara K, Hanakawa Y *et al.* (2005) Induction of keratinocyte migration via transactivation of the epidermal growth factor receptor by the antimicrobial peptide LL-37. *J Immunol* 175:4662–8

Yang D, Chertov O, Bykovskaia SN, Chen Q, Buffo MJ, Shogan J *et al.* (1999) defensins: linking innate and adaptive immunity through dendritic and T cell CCR6. *Science* 286:525–8

Yang D, Chen Q, Schmidt AP, Anderson GM, Wang JM, Wooters JO *et al.* (2000) LL-37, the neutrophil granule- and epithelial cell-derived cathelicidin, utilizes formyl peptide receptor-like 1 (FPRL1) as a receptor to chemoattract human peripheral blood neutrophils, monocytes, and T cells. *J Exp Med* 192:1069–74

Zahm JM, Debordeaux C, Raby B, Klossek JM, Bonnet N, Puchelle E (2000) Mitogenic effect of recombinant HGF on airway epithelial cells during the *in vitro* wound repair of the respiratory epithelium. *J Cell Physiol* 185:447–53

Zanetti M, Gennaro R, Romeo D (1995) Cathelicidins: a novel protein family with a common proregion and a variable C-terminal antimicrobial domain. *FEBS Lett* 374:1–5

Zhang H, Porro G, Orzech N, Mullen B, Liu M, Slutsky AS (2001) Neutrophil defensins mediate acute inflammatory response and lung dysfunction in dose-related fashion. *Am J Physiol Lung Cell Mol Physiol* 280:L947–54

Molecular Vision 2006; 12:478-84 <http://www.molvis.org/molvis/v12/a55/>
Received 6 September 2005 | Accepted 6 May 2006 | Published 11 May 2006

Proteomic analysis of soluble factors secreted by limbal fibroblasts

Shigeto Shimmura,[1,2] Hideyuki Miyashita,[1] Kazunari Higa,[2] Satoru Yoshida,[2] Jun Shimazaki,[2] Kazuo Tsubota[1,2]

[1]Department of Ophthalmology, Keio University School of Medicine, Tokyo, Japan; [2]Department of Ophthalmology and Cornea Center, Tokyo Dental College, Chiba, Japan

Purpose: To identify soluble factors selectively secreted by limbal fibroblasts as possible regulators of limbal basal epithelium.

Methods: Limbal, corneal, and conjunctival fibroblasts were first expanded in vitro in Dulbecco's modified Eagle medium containing 10% fetal bovine serum, and then maintained in serum-free medium for two weeks. Proteomic analysis of culture supernatants was done to compare differences in secreted matricellular proteins. Real time PCR and western blots were done to confirm the expression of secreted protein acid and rich in cysteine (SPARC), a protein found in abundance in extracellular proteins secreted by limbal fibroblasts. Immunohistochemistry of SPARC was done in human limbal tissue to show the spatial distribution of the protein. An adhesion assay was designed to demonstrate the effects of SPARC on an SV40 immortalized human corneal epithelial cell line (HCEC).

Results: Proteomic analysis revealed several proteins selectively secreted by limbal fibroblasts. The particular spots were identified as SPARC, vimentin, serine protease, collagen alpha 2 precursor, tissue inhibitor of metalloproteinase 2 (TIMP-2), and 5,10-methlenetetrahdrofolate reductase (FADH2). The expression of SPARC was confirmed by western blot analysis, and mRNA expression was significantly higher in limbal fibroblasts compared to central corneal fibroblasts when analyzed by real time PCR. Immunohistochemistry revealed higher distribution of SPARC in the subepithelial stroma of the limbus compared to the central cornea. The addition of 10 μg/ml murine SPARC in HCEC significantly reduced cell spreading at three h.

Conclusions: The matricellular protein SPARC is preferentially secreted by limbal fibroblasts, and may modulate intercellular adhesion of basal limbal epithelial cells.

The limbal basal epithelium has distinct characteristics compared with the corneal epithelium in the expression of several genes including increased α-integrin, ATP binding cassette protein 2 (ABCG2), and decreased keratin 3 (K3) and connexin 43 [1]. The differential expression of these markers is often raised as evidence for the presence of stem cells in the basal limbal epithelium. Accumulating evidence from clinical studies also support the limbal stem cell hypothesis, with successful ocular surface reconstruction reported by several laboratories following limbal transplantation [2,3], and more recently, cultured limbal epithelial sheet transplants [4,5]. The stromal niche is believed to modulate the phenotype of overlying epithelium, which probably involves soluble factors as well as regulation by direct contact. The plasticity of epithelial cells according to the underlying stroma was demonstrated by the use of amniotic membranes, and also by reversing epithelium/stroma combinations [6].

In order to screen for differences in secreted proteins by limbal and corneal fibroblasts, we performed 2-D PAGE (proteomic analysis) of condensed supernatants of serum-free cultured cells. After six proteins were identified, we further analyzed the distribution and function of secreted protein acidic and rich in cysteine (SPARC), also known as osteonectin. SPARC is a 43 kDa protein that contains a COOH-terminal extracellular (EC) module with two Ca^2-binding domains and a follistatin-like module shared by a family of SPARC-related genes [7]. SPARC is also expressed by corneal epithelial cells, and is believed to be involved in the wound healing process of both the epithelium and stroma of the cornea [8,9]. In addition, SPARC modulates cell growth and adhesion of vascular endothelial cells [10], and has been reported to promote cancer cell migration and invasion [11]. Several of these physiological functions reported in SPARC are consistent with properties expected of soluble factors in the stromal niche of the limbus. Epithelial cell precursors are believed to be less dependent on intercellular communication, which in turn maintain these cells in an undifferentiated state. Evidence for this is given by the limited expression of the gap junctional protein, connexin 43, in basal limbal epithelial cells [1]. We therefore hypothesized that SPARC secreted constitutively by limbal fibroblasts can regulate epithelial cell adhesion.

Correspondence to: Shigeto Shimmura, MD, Department of Ophthalmology, Keio University School of Medicine, 35 Shinanomachi, Shinjuku, Tokyo 160-8582, Japan; Phone: +81-3-3353-1211; FAX: +81-3-3359-8302; email: shige@sc.itc.keio.ac.jp

METHODS

Materials: Mouse recombinant SPARC and fibronectin were purchased from Sigma-Aldrich (St. Louis, Mo). Chemicals for proteomic analysis were obtained from Wako Pure Chemical Industries (Osaka, Japan) unless otherwise noted. The SV40 transformed immortalized human corneal epithelial cell line (HCEC) was a kind gift from Dr. Kaoru Araki-Sasaki (Kagoshima Miyata Eye Clinic, 1-5-1, Nishida, Kagoshima, Japan) [12].

Cell culture and adhesion assay: Human donor corneas not suitable for transplantation were obtained from the Northwest Lions Eye Bank. The epithelium and endothelium were bluntly removed with a gill knife, and stromal tissues were cut into small segments (approximately 2 mm x 2 mm) to allow fibroblasts to migrated during culture. Fibroblasts were cultured in Dulbecco's modified Eagle medium (DMEM) medium containing 10% fetal bovine serum until confluent, and then in serum-free DMEM for two weeks prior to proteomic analysis. HCECs were maintained in supplementary hormonal epithelial medium (SHEM), a 1:1 mixture of DMEM and Ham's F12 medium (DMEM/F12; Gibco, Invitrogen Corporation, Carlsbad, CA) containing 15% fetal bovine serum, insulin (5 µg/ml; Sigma-Aldrich, St. Louis, MO), cholera toxin (0.1 µg/ml; EMD Biosciences, San Diego, CA), human recombinant epidermal growth factor (10 ng/ml; Gibco), dimethyl sulfoxide (0.5%; Sigma-Aldrich), penicillin (0.7 mg/ml; Wako Pure Chemical Industries), and streptomycin (1.39 mg/ml; Wako Pure Chemical Industries).

Proteomic analysis: Supernatants from limbal, central corneal, and conjunctival fibroblasts cultured in serum-free DMEM for two weeks were collected by centrifugation. In brief, supernatants were placed in ultrafiltration tubes (Vivaspin 20; Sartorius, Goettingen, Germany) and centrifuged (MX-300; Tomy Seiko Co., Tokyo Japan) to remove proteins with molecular weights of less than 3 kDa. Lysis buffer (8 M urea, 2% NP-40, 2% ampholine (pH3.5-10), 5% 2-ME, protease inhibitor) was then added to the supernatant, and centrifugation was repeated. Two-dimensional PAGE was performed as previously described in the literature [13]. In brief, the first dimension was based on isoelectric focusing (pH 3.5-10) using a disk gel (Nihon Eido, Tokyo, Japan), followed by the second dimension done by SDS-PAGE in a 16.8% acrylamide gel (Bio-Rad Laboratories, Hercules, CA). Protein spots were visualized by Coomassie brilliant blue (CBB). Selected spots were dissected and digested with trypsin in 0.1 M ammonium hydrogen carbonate containing 10% acetonitrile for 16 h at 37 °C. Peptides were extracted from the gels with 60% acetonitrile containing 0.1% trifluoroacetic acid and then vortexed for 30 min. Peptide fragments were separated by C18 column (Magic C18 P/N 902-61260-00; AMR Inc., Tokyo, Japan) in a linear gradient (5-60%) of acetonitrile containing 0.1% formic acid. Separated peptides were analyzed by ion-trap mass spectrometry (MS, LCQ DECA; Thermoquest Corp., San Jose, CA) using a nanospray ionization apparatus. MS data analysis was done using Sequest (Thermoquest) and the Mascot Internet version [14].

Western blot: Western blot was used to confirm the expression of SPARC by cultured limbal and corneal fibroblasts, as well as primary cultured corneal epithelial cells. Culture supernatants were collected after two weeks of culture in DMEM containing 10% FBS and stored without condensation for western blot analysis. Cell pellets were dissolved with lysis buffer (50 mM Tris-HCl, pH7.4, 150 mM NaCl, 1% Nonidet P-40) and homogenized. Samples were incubated for 40 min at 4 °C, and then centrifuged at 15,000 rpm for 30 min

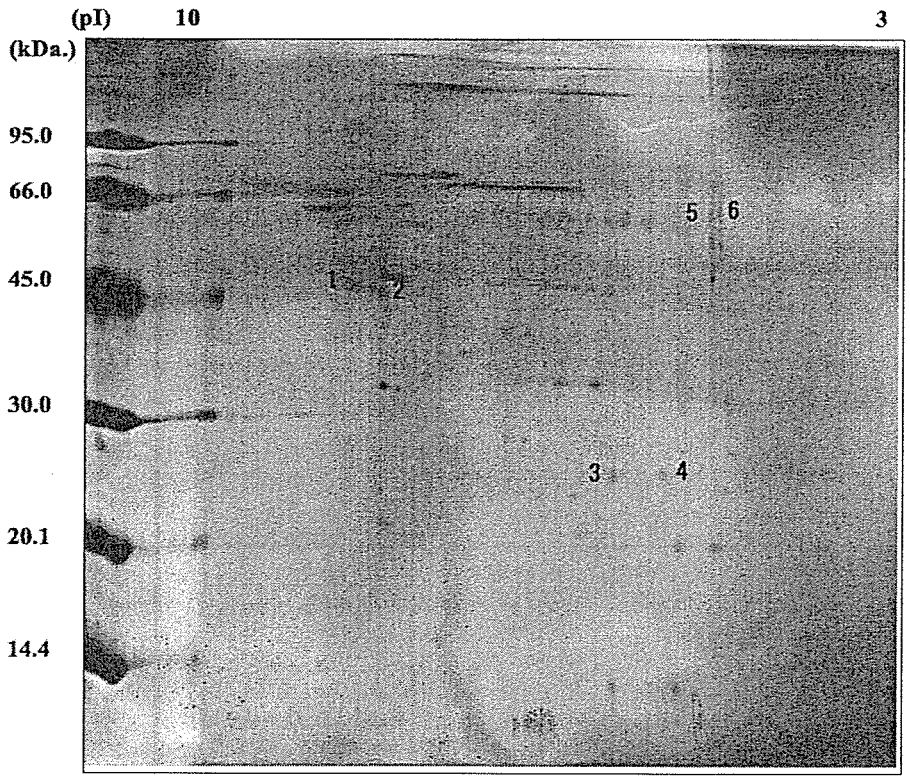

Figure 1. 2-D PAGE of proteins concentrated from the supernatant of limbal fibroblasts. Spots were visualized with Coomassie brilliant blue. Six spots (numbered) were found to be distinctively expressed by limbal fibroblasts and were identified by ion-trap mass spectrometry. The name and GenBank accession number for each protein are listed in Table 1.

at 4 °C. Protein concentration of the supernatant was determined by the DC protein assay (Bio-Rad Lab). All samples were then diluted in 2X sample buffer (100 mM Tris-HCl, pH 6.8, 4% SDS; Gibco, Invitrogen, Carlsbad, CA), 20% Glycerol (Wako), 12% 2-mercaptoethanol (Wako) and boiled. Ten µg of each sample (5 µg for β-actin) were loaded on a Novex NuPAGE 10% Bis-Tris gel (Invitrogen) and transferred onto polyvinylidene difluoride (PVDF) membranes (Millipore, Billerica, MA). Membranes were blocked with 5% skim milk (Difco Laboratories, Detroit, MI) and 1.5% normal donkey serum in PBS for 60 min at room temperature. Membranes were reacted with an anti-SPARC antibody (1.B.789; US Biological, Swampscott, MA) for 60 min at room temperature. After three washes in TBST, donkey biotinylated antimouse IgG (Jackson ImmunoResearch) was added for 30 min at room temperature. Protein bands were visualized by the Vectastain ABC Elite Kit (Vector Laboratories, Bulingame, CA) using DAB (Vector Laboratories) as a substrate.

Real-time polymerase chain reaction: Total RNA was isolated from cultured limbal and corneal fibroblasts using the SV total RNA isolation system (Promega Co., Madison, WI) according to the manufacturer's recommendations. cDNA was prepared from total RNA with oligo (dT) priming and AVM reverse transcriptase XL (Takara, Bio Inc., Shiga, Japan) by incubation of a 25 µl mixture at 41 °C for 1 h. cDNA was subjected to PCR using the gene specific oligonucleotide primers and probe (5'-ACC CCA TTG ACG GGT ACC TCT CCC A-3'). Real-time reverse transcriptase polymerase chain reaction (real-time RT-PCR) using TaqMan chemistry (Applied Biosystems, Foster City, CA) and the ABI Prism 7700 Sequence Detection System (Applied Biosystems) was used to semiquantitate SPARC expression in limbal, corneal, and conjunctival fibroblasts. PCR products were detected during the exponential phase of the reaction in order to semiquantitate SPARC expression by each cell type (n=3).

Immunohistochemistry: Frozen sections prepared from a donor human cornea embedded in 4% carboxymethyl cellulose (CMC; Finetec Co., Ltd., Japan) were fixed in 4% paraformaldehyde (PFA) for 10 min. The fixed sections were

Table 1.

Protein	Accession number	Spot number
secreted protein, acidic, cysteine-rich (SPARC); Osteonectin(secreted protein, acidic, cysteine-rich)	NP_003109	1
Vimentin	AAA61279	2
tissue inhibitor of metalloproteinases-2	AAC50729	3
Human Collagen alpha2(I) chain precursor	P08123	4
serine protease, Homo sapiens	AAC97211	5
5,10-methylenetetrahydrofolate reductase (FADH2; EC 1.7.99.5)	S46454	6

Proteins that were detected in the supernatant of limbal fibroblasts, but not from central corneal fibroblasts in the proteomic analysis.

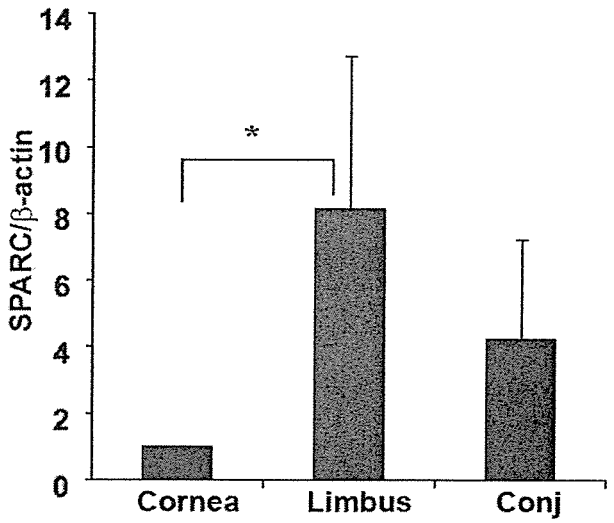

Figure 2 . Real time PCR comparing mRNA expression of SPARC in cultured limbal, corneal, and conjunctival fibroblasts. Data is expressed as SPARC expression by corneal fibroblasts as 1 unit. Limbal fibroblasts expressed a signficantly higher level of SPARC compared to the central cornea (n=3). The asterisk indicates a $p<0.05$.

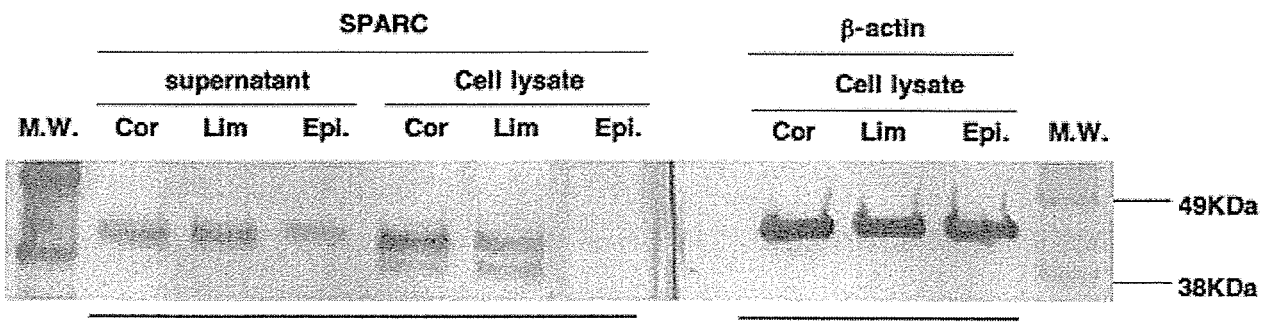

Figure 3. Western blot analysis of SPARC in culture supernatants and cell lysates of corneal and limbal fibroblasts, and primary corneal epithelial cells. Limbal fibroblasts secreted higher levels of SPARC protein compared with corneal fibroblasts. SPARC was also detected from primary epithelial cell cultures.

treated with liberate antibody binding solution (L.A.B.; Polyscience, Inc., Warrington, PA.) at room temperature for 15 min for antigen retrieval. Antibodies used were antiosteonectin (Haematologic Technologies, Inc. Essex Junction, VT) and Cy3-labeled antimouse IgG secondary antibody. Isotype rat IgG (Chemicon) was used as control. The sections were incubated with 1 µg/ml 4',6-diamidino-2-phenylindole (DAPI; Dojindo Laboratories, Tokyo, Japan) at room temperature for 5 min. Finally, sections were washed three times in Tris-buffered saline tween (TBST) and coverslipped using an antifading mounting medium (50 mM Tris buffer saline, 90% glycerin; Wako), and 10% 1,4-diazabicyclo (2,2,2) octane (Wako).

Adhesion assay: One of the established physiological effects of SPARC is the suppression of vascular endothelial cell growth and adhesion [10]. In order to pursue the possibility that SPARC may have similar effects on corneal epithelial cells in vitro, we performed a modified version of a cell adhesion study reported previously [15]. Nontreated 96 well plates (260887, Nalge Nunc Int, Rochester, NY) were coated with 100 µl of fibronectin in phosphate-buffered saline plus (PBS+; 1 µg/ml) at 4 °C overnight, and washed with PBS. Serum-free DMEM with or without murine SPARC (final 10 µg/ml) were added to the wells. HCEC were trypsinized, neutralized, resuspended in serum-free DMEM, and a 50 µl sample was added to each well (10^4/well). After 3 h incubation at 37 °C, the central area of each well (856 µm x 678 µm) was photographed using the Axiovert 200 microscope (x10, Carl Zeiss, Gottingen, Germany). Cells were scored as previously described [16]. Round cells with no apparent signs of spreading were given a score of 3. Rounded cells with short cellular processes were assigned a score of 2. Spread, flattened cells were given a score of 1. Adhesion score for each well was calculated by the average score of all visible cells in a randomly selected field of view.

RESULTS

Proteomic analysis: 2-D PAGE of supernatant from limbal fibroblasts is shown in Figure 1. Total protein levels were low, in general, since this was an analysis of culture supernatants and not of homogenized cells. Although samples were condensed prior to electrophoresis, only blots that were dense enough to allow sequence analysis were further investigated. The six proteins specifically identified in the supernatant of limbal fibroblasts along with their accession numbers are listed in Table 1.

Constitutive expression of SPARC by limbal fibroblasts: We further pursued the possible role of SPARC as a major matricellular protein in the limbal stroma. Real-time PCR was done to semiquantitate SPARC mRNA transcription in cultured cells, and the result was consistent with the higher protein content in limbal fibroblasts observed in the proteomic analysis (Figure 2). Western blot results confirmed SPARC protein secreted in the supernatant of limbal and corneal fibroblasts (Figure 3). SPARC was also expressed by primary corneal epithelial cells, however, the expression levels were lower compared to limbal and corneal fibroblasts.

Immunohistochemistry: The cumulative data show higher expression of SPARC in limbal fibroblasts in vitro, but does not necessarily reflect that this applies in vivo. We therefore performed immunohistology using an anti-SPARC monoclonal antibody in fresh donor limbal tissue to observe the distribu-

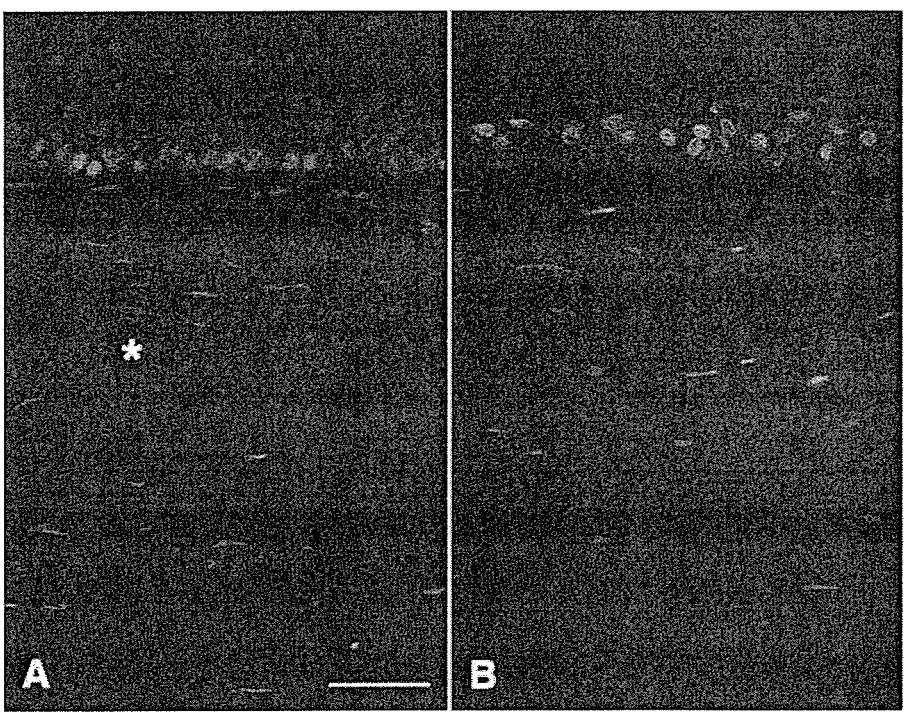

Figure 4. Immunohistology of a corneolimbal segment using an anti-SPARC monoclonal antibody. The subepithelial tissue in the limbus (**A**) showed SPARC distributed in the interstitial space (asterisk). SPARC-associated signals were much lower in the central cornea (**B**). The scale bar represents 50 µm.

tion of SPARC in situ. As shown in Figure 4A, a higher level of SPARC-associated Cy-3 fluorescence was observed in the subepithelial regions of the limbus compared with the central cornea. The difference can be appreciated when compared with the uniform fluorescence observed in the overlying epithelial cells (Figure 4B). Thus, SPARC is constitutively expressed in the limbal stroma by resident fibroblasts without the stimulation of a wound healing process.

Cell adhesion assay: In order to observe the effects of SPARC on corneal epithelial cells in vitro, an immortalized cell line (HCEC) were used to observe for changes in cell adhesion and morphology. The addition of SPARC in the culture supernatant resulted in rounding of individual HCEC after 3 h (Figure 5). The difference was statistically significant using a rounding index originally described by Lane and Sage [16] (n=5).

DISCUSSION

SPARC is a 43 kDa protein that contains a COOH-terminal EC module with two Ca^{2+}-binding domains, a follistatinlike module, and an NH_2-terminal acidic module [7]. The expression of SPARC by corneal stromal cells has been reported to play a role in the wound healing response, evidenced by the upregulation of SPARC by the fibroblast and myofibroblast phenotype [9]. However, SPARC was not detected in quiescent corneal stromal cells, and hence, the major function of the protein was speculated to be related to wound healing. Conversely, SPARC secreted by epithelial cells was shown to induce contraction of stromal fibroblasts in vitro, suggesting that SPARC is a key protein in epithelial/stromal interaction of the cornea [17]. SPARC has also been proposed to be involved in corneal epithelial migration and stratification following mechanical ablation [8].

We found that limbal fibroblasts secreted higher levels of SPARC compared to central corneal fibroblasts in vitro without stimulation by serum or cytokines, and also in vivo without any wound-healing stimuli. SPARC was one of only a few proteins detectable by proteomic analysis in the limbal fibroblast supernatant, suggesting a functional role in the homeostasis of the limbal structure. Although it can be argued that corneal fibroblasts cultured in vitro are not the same as keratocytes in vivo, experiments requiring large quantities of cells would not be possible without in vitro expansion. All cells used in the current study were first expanded in vitro using serum containing 10% serum, therefore, the phenotype of these cells at the time of analysis is not necessarily consistent with the normal phenotype. The results of preotomics alone, therefore, have limits without further analysis. Inter-

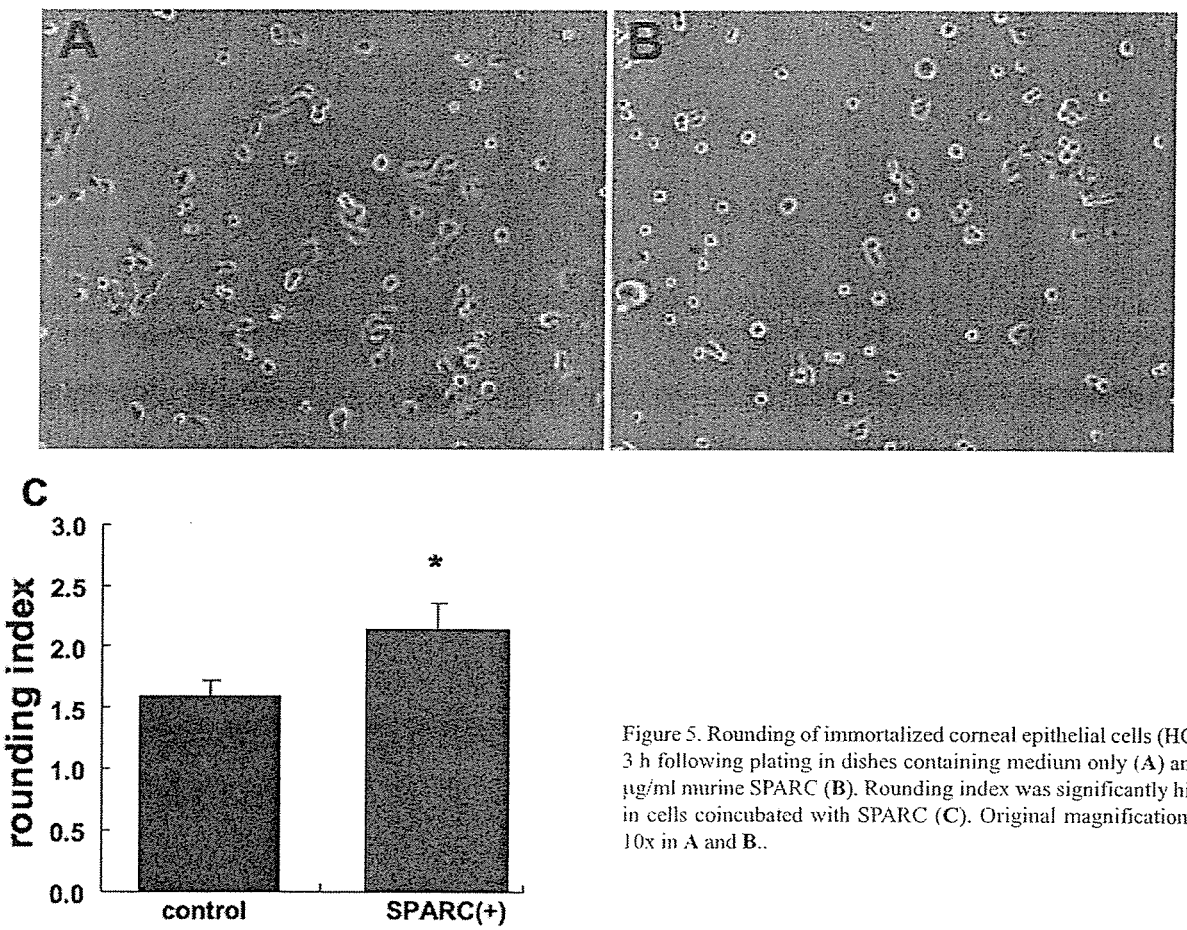

Figure 5. Rounding of immortalized corneal epithelial cells (HCEC) 3 h following plating in dishes containing medium only (**A**) and 10 µg/ml murine SPARC (**B**). Rounding index was significantly higher in cells coincubated with SPARC (**C**). Original magnification was 10x in **A** and **B**..

estingly, one of the proteins detected in the limbal cell supernatant was vimentin, an intracellular intermediate fiber, suggesting that some of the proteins in the supernatant may have been the result of apoptosis. We did not pursue this issue further, and chose to focus on SPARC which is a secreted protien.

Figure 4 shows the immunohistochemistry of SPARC in donor cornea tissue. The result shows that SPARC is expressed more in the limbal stroma, reflecting the results of real time RT-PCR and western blots of cell supernatants. We have also found through immunohistochemistry that epithelial cells were positive for SPARC, while western blots only detected trace levels of SPARC from cell lysates and supernatant of primary cultured epithelial cells. This may be explained by the fact that SPARC is secreted by corneal epithelial cells during wound repair [8,17], and that primary cells in vitro may be in a state similar to epithelial cells undergoing wound healing.

We focused on the function of SPARC, since the matricellular protein has been reported to regulate the adhesion of bovine aortic endothelial cells [10]. Using a previously described adhesion assay, we found that exogenous SPARC inhibited adhesion of a human corneal epithelial cell line, which may be due to the Ca^{2+}-binding ability of SPARC. Espana et al. [6] have previously reported that limbal stroma, and not corneal stroma, was required to maintain an undifferentiated phenotype (K3 negative, Cx 43-low) in corneal epithelial cell sheets. This implies that soluble factors expressed by limbal fibroblasts may be involved in this phenomenon. The extracellular matrix and basement membrane components of the limbal area are distinct from the central cornea, as reported by several studies [18,19]. SPARC is also involved in the migration and invasion of prostate cancer cells [11] and breast cancer cells [20] through the activation of matrix metalloproteinase 2 (MMP2). These are several properties that are expected of matricellular proteins in the putative limbal stem cell niche. Interestingly, the MMP2-specific inhibitor, TIMP2 was also preferentially detected in the supernatant of limbal fibroblasts, suggesting that an intricate network based on a balance of effectors and inhibitors may be involved in the homeostasis of the limbal stem cell niche.

Growth factors such as keratinocyte growth factor and hepatocyte growth factor are also mediators of fibroblast/epithelial interaction involved in epithelial proliferation and migration [21]. Although the network of epithelial/mesenchymal interaction in the corneal limbus is sure to involve a wide variety of matricellular proteins, cytokines, and growth factors, the inhibition of cellular adhesion and cell/cell interaction by SPARC may be a major component of the limbal microenvironment. We found that the human amniotic membrane (AM) also contains SPARC (data not shown), which may partially explain the ability of AM to preserve the undifferentiated state of limbal epithelial cell in vitro [22]. While further studies are required to elucidate the interactions of soluble factors involved in the limbal niche, a combination of such components may be used to enrich limbal stem cells in vitro.

ACKNOWLEDGEMENTS

This study was partly supported by a grant of Advanced and Innovational Research Program in Life Sciences from the Ministry of Education, Culture, Sports, Science and Technology of Japan.

REFERENCES

1. Chen Z, de Paiva CS, Luo L, Kretzer FL, Pflugfelder SC, Li DQ. Characterization of putative stem cell phenotype in human limbal epithelia. Stem Cells 2004; 22:355-66.
2. Kenyon KR, Tseng SC. Limbal autograft transplantation for ocular surface disorders. Ophthalmology 1989; 96:709-22; discussion722-3.
3. Tsubota K, Satake Y, Kaido M, Shinozaki N, Shimmura S, Bissen-Miyajima H, Shimazaki J. Treatment of severe ocular-surface disorders with corneal epithelial stem-cell transplantation. N Engl J Med 1999; 340:1697-703.
4. Koizumi N, Inatomi T, Suzuki T, Sotozono C, Kinoshita S. Cultivated corneal epithelial transplantation for ocular surface reconstruction in acute phase of Stevens-Johnson syndrome. Arch Ophthalmol 2001; 119:298-300.
5. Pellegrini G, Traverso CE, Franzi AT, Zingirian M, Cancedda R, De Luca M. Long-term restoration of damaged corneal surfaces with autologous cultivated corneal epithelium. Lancet 1997; 349:990-3.
6. Espana EM, Kawakita T, Romano A, Di Pascuale M, Smiddy R, Liu CY, Tseng SC. Stromal niche controls the plasticity of limbal and corneal epithelial differentiation in a rabbit model of recombined tissue. Invest Ophthalmol Vis Sci 2003; 44:5130-5.
7. Brekken RA, Sage EH. SPARC, a matricellular protein: at the crossroads of cell-matrix communication. Matrix Biol 2001; 19:816-27.
8. Latvala T, Puolakkainen P, Vesaluoma M, Tervo T. Distribution of SPARC protein (osteonectin) in normal and wounded feline cornea. Exp Eye Res 1996; 63:579-84.
9. Berryhill BL, Kane B, Stramer BM, Fini ME, Hassell JR. Increased SPARC accumulation during corneal repair. Exp Eye Res 2003; 77:85-92. Erratum in: Exp Eye Res 2003; 77:643.
10. Sweetwyne MT, Brekken RA, Workman G, Bradshaw AD, Carbon J, Siadak AW, Murri C, Sage EH. Functional analysis of the matricellular protein SPARC with novel monoclonal antibodies. J Histochem Cytochem 2004; 52:723-33.
11. Jacob K, Webber M, Benayahu D, Kleinman HK. Osteonectin promotes prostate cancer cell migration and invasion: a possible mechanism for metastasis to bone. Cancer Res 1999; 59:4453-7.
12. Araki-Sasaki K, Ohashi Y, Sasabe T, Hayashi K, Watanabe H, Tano Y, Handa H. An SV40-immortalized human corneal epithelial cell line and its characterization. Invest Ophthalmol Vis Sci 1995; 36:614-21.
13. Kajiwara H, Kaneko T, Ishizaka M, Tajima S, Kouchi H. Protein profile of symbiotic bacteria Mesorhizobium loti MAFF303099 in mid-growth phase. Biosci Biotechnol Biochem 2003; 67:2668-73.
14. Perkins DN, Pappin DJ, Creasy DM, Cottrell JS. Probability-based protein identification by searching sequence databases using mass spectrometry data. Electrophoresis 1999; 20:3551-67.
15. Girard JP, Springer TA. Modulation of endothelial cell adhesion by hevin, an acidic protein associated with high endothelial venules. J Biol Chem 1996; 271:4511-7.

16. Lane TF, Sage EH. Functional mapping of SPARC: peptides from two distinct Ca+(+)-binding sites modulate cell shape. J Cell Biol 1990; 111:3065-76.
17. Mishima H, Hibino T, Hara H, Murakami J, Otori T. SPARC from corneal epithelial cells modulates collagen contraction by keratocytes. Invest Ophthalmol Vis Sci 1998; 39:2547-53.
18. Ljubimov AV, Burgeson RE, Butkowski RJ, Michael AF, Sun TT, Kenney MC. Human corneal basement membrane heterogeneity: topographical differences in the expression of type IV collagen and laminin isoforms. Lab Invest 1995; 72:461-73.
19. Fukuda K, Chikama T, Nakamura M, Nishida T. Differential distribution of subchains of the basement membrane components type IV collagen and laminin among the amniotic membrane, cornea, and conjunctiva. Cornea 1999; 18:73-9.
20. Gilles C, Bassuk JA, Pulyaeva H, Sage EH, Foidart JM, Thompson EW. SPARC/osteonectin induces matrix metalloproteinase 2 activation in human breast cancer cell lines. Cancer Res 1998; 58:5529-36.
21. Li DQ, Tseng SC. Three patterns of cytokine expression potentially involved in epithelial-fibroblast interactions of human ocular surface. J Cell Physiol 1995; 163:61-79.
22. Grueterich M, Espana EM, Tseng SC. Ex vivo expansion of limbal epithelial stem cells: amniotic membrane serving as a stem cell niche. Surv Ophthalmol 2003; 48:631-46.

The print version of this article was created on 11 May 2006. This reflects all typographical corrections and errata to the article through that date. Details of any changes may be found in the online version of the article.

SCIENTIFIC REPORT

Microkeratome assisted deep lamellar keratoprosthesis

S Shimmura, H Miyashita, Y Uchino, T Taguchi, H Kobayashi, J Shimazaki, J Tanaka, K Tsubota

Br J Ophthalmol 2006;**90**:826–829. doi: 10.1136/bjo.2006.090324

Aims: To establish a keratoprosthesis (Kpro) surgical technique that maintains an intact superficial corneal layer.
Methods: A manual microkeratome (Moria LSK-1) was used to create a 130 μm flap of approximately 10 mm diameter in the right eye of Japanese white rabbits. The stoma beneath the flap area was dissected before the removal of a 5.0 mm stromal disc. A 5.0 mm collagen I immobilised poly(vinyl alcohol) (COL-PVA) disc was placed on the exposed posterior stroma close to Descemet's membrane. The flap was repositioned and fixed using 10-0 nylon sutures, which were removed 2 days following surgery. The corneas were followed clinically by slit lamp microscopy and photographs. Rabbits were sacrificed after 6 months, and the transplanted corneas were examined histologically by haematoxylin and eosin staining and immunohistochemistry against vimentin and α-smooth muscle actin (α-SMA).
Results: The transplanted COL-PVA discs remained transparent throughout the study, with no complications related to the flap or overlying epithelium. The interface between COL-PVA and Descemet's membrane remained clear without signs of opacification caused by scarring or cellular deposition. Pathology revealed the intact COL-PVA polymer in the posterior stroma, with minimal cellular infiltration along the anterior and posterior interfaces. Immunohistology shows vimentin and α-SMA staining at levels comparable to lamellar keratoplasty control.
Conclusions: Microkeratome assisted deep lamellar keratoprosthesis may be a safe technique for the transplantation of artificial hydrogels for therapeutic purposes.

The search for an ideal artificial cornea has a long history, which has led to the development of several keratoprosthesis (Kpro), some of which are already in clinical use.[1–6] The Dohlman-Doane[7] and AlphaCor[8] Kpros are the two models currently approved by the Food and Drug Administration, and clinical studies are accumulating. The material used for Kpros should be biocompatible to the extent that excessive inflammation and scarring do not occur at the anterior and posterior interfaces of the visual axis. In order to preserve an optically clear interface, several Kpros are designed so that the corneal epithelium does not cover the anterior surface. Although satisfactory vision is achieved with a successful Kpro implant, a discontinuous epithelial layer may lead to pigment deposition or extrusion of the Kpro.[6] In order to circumvent such complications, a strategy to integrate biological components to increase biocompatibility was adopted in the development of corneal equivalents.[8 9] Corneal equivalents show characteristics similar to the natural cornea in vitro, however, a prototype that lasts indefinitely in vivo is yet to be designed.

The need for corneal equivalents is based on the assumption that healthy components of the epithelium, stroma, and corneal nerves are required to reconstitute the cornea. However, several studies have shown that artificial materials are stable when placed in stromal pockets, as long as stromal tissue and nerves are left intact in the remaining cornea. The presence of healthy stromal keratocytes is of importance in maintaining a healthy epithelial layer because of the many soluble factors exchanged by both tissue in an elaborate epithelial stromal "cross talk."[10] An intact epithelium with an underlying stromal layer in laser in situ keratomileusis (LASIK) flaps may explain the fewer incidences of haze observed in LASIK compared with photorefractive keratectomy (PRK).[11–13]

Opacification of the posterior stromal interface is also occasionally observed in Kpro surgery. Retrocorneal membranes are associated with Kpros that have posterior optics projecting directly into the anterior chamber,[14] and retroprosthetic membranes occur in approximately 9% of patients with the AlphaCor Kpro.[15] In either case, opacification can be minimised if activation of fibroblasts can be suppressed by physical or pharmacological means. From our experience with deep lamellar keratoplasty (Dro), we have found that by dissecting directly down to the Descemet's membrane (DM), interlamellar opacification following surgery is minimal. We therefore hypothesised that if Kpros can be transplanted directly onto the deep stroma, while leaving anterior stromal tissue intact beneath the epithelium, such a surgical technique may allow for a long standing artificial device. In order to achieve this architecture, we combined the use of a microkeratome with a D surgical technique already in clinical use.[16 17] The technique is similar to the microkeratome assisted posterior keratoplasty described by two different groups[18 19] without penetrating into the anterior chamber. In this report, we show the macroscopic and histological results of poly(vinyl alcohol) (PVA) discs transplanted in rabbits using this "microkeratome assisted deep lamellar Kpro" technique, which showed promising mid-term results.

MATERIAL AND METHODS

PVA implants

Collagen I was immobilised to PVA (PVA-COL) as previously described.[20] In brief, PVA powder was dissolved in a mixture of dimethyl sulfoxide (DMSO) water solvent and was allowed to stand at −20°C for 24 hours to form a gel. The surface of the gel was modified with hexamethylene dissocyantate (HMDI), which was then immersed in type I collagen solution (porcine skin, 0.5 mg/ml, Nitta Gelatin Co Ltd, Osaka, Japan). PVA-COL was prepared as a non-porous hydrogel, with a water content of 78% to 80%, which is similar to the host cornea. PVA-COL discs (200 μm thickness, 5.0 mm diameter) were sterilised before surgery.

Abbreviations: α-SMA, α-smooth muscle actin; BSA, bovine serum albumin; COL-PVA, collagen I immobilised poly(vinyl alcohol); DLKPro, deep lamellar keratoprosthesis; DM, Descemet's membrane; DMSO, dimethyl sulfoxide; HE, haematoxylin and eosin; HMDI, hexamethylene dissocyantate; Kpro, keratoprosthesis; LKP, lamellar keratoplasty; LASIK, laser in situ keratomileusis; PBS, phosphate buffered saline; PRK, photorefractive keratectomy; PVA, poly(vinyl alcohol)

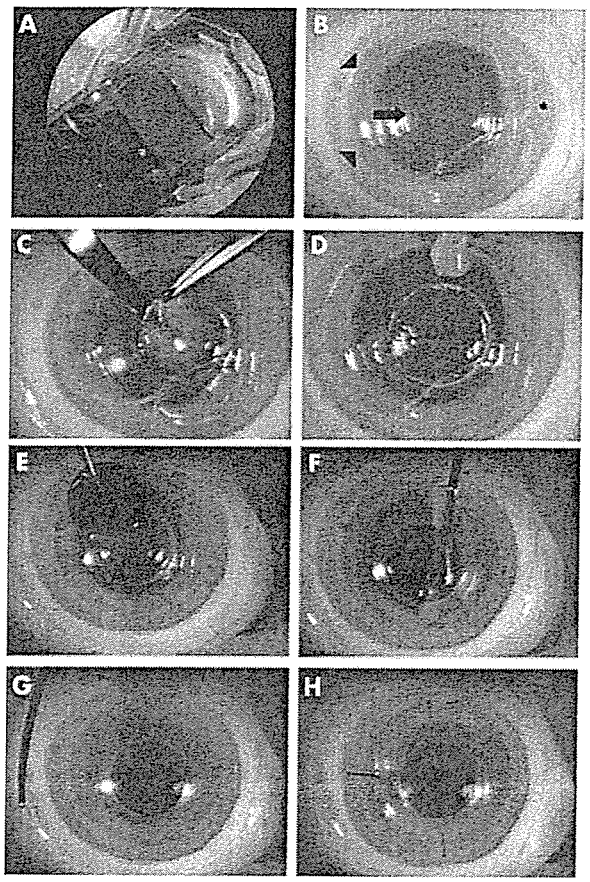

Figure 1 Demonstration of DLKPro surgical technique using an enucleated rabbit eye. (A) A manual microkeratome is used to create a hinged flap. (B) A 5 mm incision (arrow) is trephined under the lifted flap (*). Arrowheads indicate the margin of the flap bed. Air is injected into the anterior chamber to allow visualisation of Descemet's membrane (see text for details). (C, D) Stromal tissue is removed using a lamellar knife to reveal Descemet's membrane (DM). (E–H) A 5.0 mm PVA disc (stained with trypan blue to enhance visibility) is inserted into the excised wound, and the flap is repositioned and fixed using three to five 10-0 nylon sutures.

Surgical procedure

All animals were treated according to the ARVO statement for the use of animals in ophthalmology and vision research. Female Japanese white rabbits (n = 6, 3 kg body weight, Shiraishi experimental animal breeding farm, Tokyo, Japan) were anaesthetised with 4 ml intramuscular ketamine and xylazine (1:7 mixture), as well as topical xylocaine at the start of surgery. Two rabbits were used as lamellar keratoplasty () control, and four rabbits underwent the study procedure. A 130 μm flap with a nasal hinge was created using the LSK-1 microkeratome (Moria, Antony, France). After the flap was lifted, a manual trephine (5.0 mm diameter) was used to create an incision extending into the deep stroma without perforating the DM. Air was injected into the anterior chamber, and the DM was dissociated from the posterior stromal surface using a blunt spatula as previously described for deep lamellar keratoplasty (DLKP).[17] Air injection into the anterior chamber was first described by Melles *et al*, which allows visualisation of incision depth reducing the risk of perforating DM.[16] The trephined stromal disc was then removed using micro scissors and forceps to remove any remaining stromal strands. The PVA-COL disc was then placed into the circular space without any suture fixation. The flap was repositioned and fixed with 5 10-0 nylon sutures. A summary of the surgical procedure is presented in figure 1.

Flap sutures were removed 2 days following surgery after confirming that the corneal epithelium was intact. Topical antibiotics and steroids were applied twice daily for 1 week. One of the rabbits in the study group experienced flap complications (thin flaps, suture related infections), therefore, a total of three rabbits were observed and photographed for up to 6 months following surgery. One rabbit each was sacrificed after 1 month, 3 months, and 6 months with an overdose of pentobarbital, and the corneas with implants were excised and fixed for histological and immunohistochemical analysis.

Histological analysis

Corneas were fixed in 10% formalin neutral buffer solution (Mildform 10N, Wako Pure Chemical Industries, Osaka, Japan) at 4°C overnight, and then embedded in paraffin. Four μm sections were stained with haematoxylin and eosin (HE) or immunostained with primary antibodies against α-smooth muscle actin (α-SMA, clone 1A4, 0.2 μg/ml, Neomarkers, Lab Vision Corporation, Fremont, CA, USA) and vimentin (clone V9, 0.2 μg/ml, Neomarkers). In brief, sections were rehydrated, treated with 3% H_2O_2, blocked with phosphate buffered saline (PBS) containing 10% normal goat serum and 1% bovine serum albumin (BSA), and treated with primary antibody at 4°C overnight. After washing, sections were incubated with biotinised goat anti-mouse IgG1 (0.5 μg/ml, Southern Biotechnology Associates Inc, Birmingham, AL, USA) or anti-mouse IgG2 (Santa Cruz Biotechnology, Santa Cruz, CA, USA), treated with ABC kit (Vector Laboratories Inc, Burlingame, CA, USA), and ABC is detected by diaminobenzidine (DAB) kit (Vector Laboratories Inc).

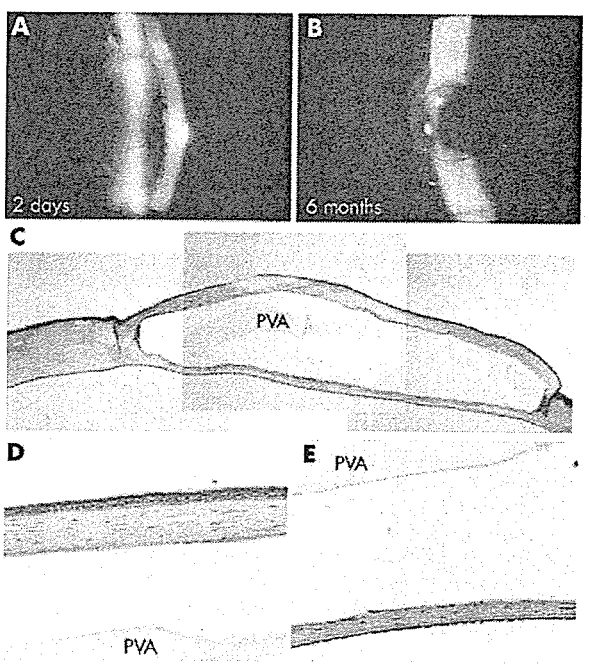

Figure 2 Surgical results of DLKPro. Postoperative slit photographs 2 days (A, ×22) and 6 months (B, ×16) following surgery. HE staining of the same cornea shows an intact disc within the stroma with minimal cellular infiltration (C). High magnification of the flap (D) and posterior stroma (E) shows no cellular infiltration. The space between stroma and implant is an artefact of tissue fixation. PVA = PVA implant.

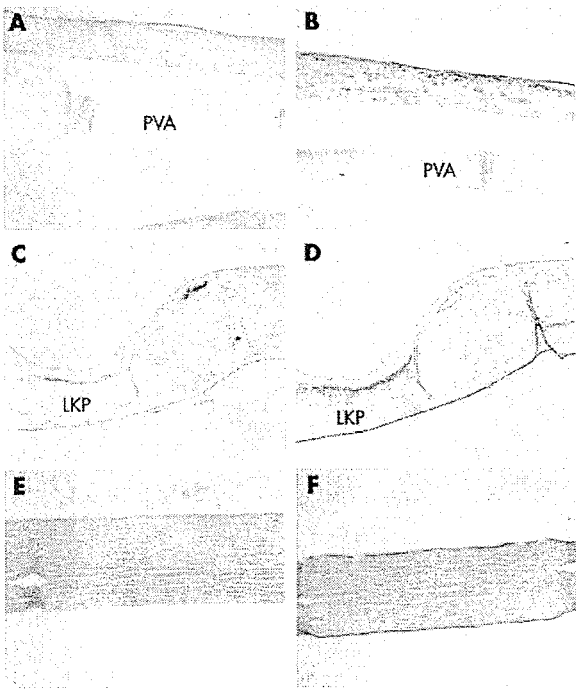

Figure 3 Immunohistochemistry against α-SMA (A) shows minimal staining compared with the lamellar keratoplasty control (C), indicating the absence of myofibroblasts. Vimentin (B) is expressed locally beneath the epithelium similar to LKP control (D) representing activated fibroblasts. (E, F) Normal control cornea stained with anti-αSMA (E) and anti-vimentin (F).

RESULTS

Figure 2A shows the PVA-COL implant positioned beneath the sutured flap 2 days following surgery. The epithelium was smooth and intact, with no inflammation of the ocular surface and anterior chamber. The polymer stromal interface was smooth in both the anterior and posterior surfaces for up to 6 months (fig 2B). Minimal scarring was found along the circumference of the PVA-COL disc, and the ocular surface was quiet without signs of inflammation or infection throughout the entire follow up period.

Haematoxylin and eosin stains of the cornea shows the intact polymer without signs of melting or cellular infiltration after 6 months (fig 2C). A thin layer of stroma is found beneath the disc and DM, which may represent either residual stroma at the time of surgery, or regenerated tissue during the observation period (fig 2E). The epithelium of the flap overlying the polymer is stratified without any pathological signs of thinning or erosions (fig 2D). Immunohistochemistry using an anti-α-SMA (fig 3A) shows that keratocyte (fibroblast) activation is minimal at the polymer-stromal interfaces, which is consistent with the minimal scarring observed by slit lamp examination. There was a slight increase in vimentin positive cells in the flap (fig 3B) compared to normal cornea control (fig 3F), indicating that some of the keratocytes were of the fibroblast phenotype. However, the appearance of fibroblastic cells is common in corneal surgery, as shown in a rabbit with an autologous lamellar transplant (fig 3D).

DISCUSSION

Previous attempts at using artificial polymers as transplantable grafts have often encountered problems with extrusion and infection.[21 22] An intact ocular surface may be a way to prevent these complications; however, long term maintenance of a stratified epithelial layer over an artificial hydrogel has proved difficult for extended periods in vivo.[9] The reason why such polymers, which often support stratified epithelium in vitro,[23] fail to maintain a healthy epithelium in vivo can be explained by a lack of stromal cells that are involved in the homeostasis of the epithelium.[10] The surgical technique described in this report makes use of residual stroma within the flap to function both as a mechanical barrier against polymer extrusion, as well as a reservoir of keratocytes for the maintenance of the overlying epithelium. The structure of the anterior stroma is similar to the AlphaCor implant before the stage II procedure in cases without the Gunderson conjunctival flap. As shown from the histology of the implanted cornea after 6 months, keratocytes are observed between the polymer and epithelium, and the appearance of the overlying epithelium is normal without signs of mechanical stress or malnutrition. The COL-PVA hydrogel used for the implant has already been shown to maintain a normal glycogen content in overlying epithelium demonstrated by PAS staining.[20]

Another vital property of keratoprosthesis is the optical clarity achieved along the visual axis after implantation. Therefore, conventional full thickness keratoprosthesis may offer better vision when successfully managed. The advantage of the material and technique used in this study is higher biocompatibility of the keratoprosthesis that is completely implanted within the stroma. Figures 2 and 3 show that opacification of the interface is minimal, with scarring observed only along the edge of the implanted disc. Such scarring does not hinder the refraction of the cornea, and may serve to secure the polymer in position within the stroma. Figure 2 also shows residual stroma between the polymer and endothelium. Since there was no apparent opacification at the posterior surface of the implant, complete exposure of DM may not be necessary. This may be beneficial since exposing DM may be difficult in clinical cases.

Clinical indications for this procedure may be limited because of the requirement of a relatively clear anterior stroma. One such indication may be keratoconus patients with relative thickness of the central cornea. Although there may be an ethical issue with using keratoprosthesis in keratoconus patients, DLKPro may be an option before PKP using donor tissue. However, we think that another broader indication may be patients with recurring bullous keratopathy. Although a healthy endothelium is required to maintain clarity in a full thickness cornea, decreased vision as a result of stromal oedema can be substantially decreased by replacing 300–400 μm of the swelled stroma with a transparent polymer. Although visual acuity may be suboptimal, functional vision may be restored in patients who otherwise may require multiple grafts because of rejection or endothelial decompensation. Animal studies to investigate this possibility are under way.

Another advantage of this technique is the simple design of the implant, which may be constructed from modified contact lens moulds. Although the disc used in this study was flat, a curved design fit for the human cornea may be more compatible for clinical use. Custom designed discs may be used modulate postoperative refraction as well, since the overall refraction of the cornea can be modified by the curvature of the disc implanted beneath the flap. The concept of refractive correction using corneal inlays has been studied, with positive clinical results.[25 26] Although the results are only preliminary, improving surgical technique may compensate for some of the disadvantages of using non-biological materials for artificial corneas. The technique that we have described combining the use of a microkeratome with DLKP procedures offers a safe and reliable method to implant Krpos

into the deep stroma. An intact Descemet's membrane will act as a barrier to prevent dislocation of the Kpro into the anterior chamber, and may also minimise interface opacification because of the formation of retroprosthetic membranes.

Authors' affiliations
S Shimmura, H Miyashita, J Shimazaki, K Tsubota, Department of Ophthalmology, Keio University, Tokyo, Japan
T Taguchi, H Kobayashi, J Tanaka, Biomaterials Center, National Institute for Materials Science, Ibaragi, Japan
S Shimmura, Y Uchino, K Tsubota, Department of Ophthalmology, Tokyo Dental College, Chiba, Japan

This study was supported by The Advanced and Innovational Research Program in Life Sciences from the Japanese Ministry of Education, Culture, Sports, Science and Technology.

Correspondence to: Shigeto Shimmura, MD, Department of Ophthalmology, Keio University School of Medicine, 35 Shinanomachi, Shinjuku-ku, Tokyo 160-8582, Japan; shige@sc.itc.keio.ac.jp

Accepted for publication 1 March 2006

REFERENCES

1 **Chirila TV.** An overview of the development of artificial corneas with porous skirts and the use of PHEMA for such an application. *Biomaterials* 2001;**22**:3311–17.
2 **Kompa S,** Redbrake C, Langefeld S, *et al.* The Type II Aachen-Keratoprosthesis in humans: case report of the first prolonged application. *Int J Artif Organs* 2001;**24**:110–14.
3 **Kim MK,** Lee JL, Wee WR, *et al.* Comparative experiments for in vivo fibroplasia and biological stability of four porous polymers intended for use in the Seoul-type keratoprosthesis. *Br J Ophthalmol* 2002;**86**:809–14.
4 **Stoiber J,** Csaky D, Schedle A, *et al.* Histopathologic findings in explanted osteo-odontokeratoprosthesis. *Cornea* 2002;**21**:400–4.
5 **Dudenhoefer EJ,** Nouri M, Gipson IK, *et al.* Histopathology of explanted collar button keratoprostheses: a clinicopathologic correlation. *Cornea* 2003;**22**:424–8.
6 **Hicks CR,** Crawford GJ, Lou X, *et al.* Corneal replacement using a synthetic hydrogel cornea, AlphaCor: device, preliminary outcomes and complications. *Eye* 2003;**17**:385–92.
7 **Doane MG,** Dohlman CH, Bearse G. Fabrication of a keratoprosthesis. *Cornea* 1996;**15**:179–84.
8 **Griffith M,** Osborne R, Munger R, *et al.* Functional human corneal equivalents constructed from cell lines. *Science* 1999;**286**:2169–72.
9 **Shimmura S,** Doillon CJ, Griffith M, *et al.* Collagen-poly(N-isopropylacrylamide)-based membranes for corneal stroma scaffolds. *Cornea* 2003;**22**:S81–8.
10 **Wilson SE,** Mohan RR, Mohan RR, *et al.* The corneal wound healing response: cytokine-mediated interaction of the epithelium, stroma, and inflammatory cells. *Prog Retin Eye Res* 2001;**20**:625–37.
11 **Park CK,** Kim JH. Comparison of wound healing after photorefractive keratectomy and laser in situ keratomileusis in rabbits. *J Cataract Refract Surg* 1999;**25**:842–50.
12 **Wachtlin J,** Langenbeck K, Schrunder S, *et al.* Immunohistology of corneal wound healing after photorefractive keratectomy and laser in situ keratomileusis. *J Refract Surg* 1999;**15**:451–8.
13 **Vesaluoma M,** Perez-Santonja J, Petroll WM, *et al.* Corneal stromal changes induced by myopic LASIK. *Invest Ophthalmol Vis Sci* 2000;**41**:369–76.
14 **Aquavella JV,** Rao GN, Brown AC, *et al.* Keratoprosthesis. Results, complications, and management. *Ophthalmology* 1982;**89**:655–60.
15 **Hicks CR,** Hamilton S. Retroprosthetic membranes in AlphaCor patients: risk factors and prevention. *Cornea* 2005;**24**:692–8.
16 **Melles GR,** Lander F, Rietveld FJ, *et al.* A new surgical technique for deep stromal, anterior lamellar keratoplasty. *Br J Ophthalmol* 1999;**83**:327–33.
17 **Shimmura S,** Shimazaki J, Omoto M, *et al.* Deep lamellar keratoplasty (DLKP) in keratoconus patients using viscoadaptive viscoelastics. *Cornea* 2005;**24**:178–81.
18 **Busin M,** Arffa RC, Sebastiani A. Endokeratoplasty as an alternative to penetrating keratoplasty for the surgical treatment of diseased endothelium: initial results. *Ophthalmology* 2000;**107**:2077–82.
19 **Azar DT,** Jain S, Sambursky R, *et al.* Microkeratome-assisted posterior keratoplasty. *J Cataract Refract Surg* 2001;**27**:353–6.
20 **Miyashita H,** Shimmura S, Kobayashi H, *et al.* Collagen-immobilized poly (vinyl alcohol) as an artificial cornea scaffold that supports a stratified corneal epithelium. *J Biomed Mater Res B Appl Biomater* 2005;**76B**:56–63.
21 **Kobayashi H,** Ikada Y, Moritera T, *et al.* Collagen-immobilized hydrogel as a material for lamellar keratoplasty. *J Appl Biomater* 1991;**2**:261–7.
22 **Latkany R,** Tsuk A, Sheu MS, *et al.* Plasma surface modification of artificial corneas for optimal epithelialization. *J Biomed Mater Res* 1997;**36**:29–37.
23 **Choyce DP.** The correction of high myopia. *Refract Corneal Surg* 1992;**8**:242–5.
24 **Werblin TP,** Peiffer RL, Binder PS, *et al.* Eight years experience with Permalens intracorneal lenses in nonhuman primates. *Refract Corneal Surg* 1992;**8**:12–22.

Ocular Surface Epithelial Cells Up-Regulate HLA-G When Expanded In Vitro on Amniotic Membrane Substrates

Kazunari Higa, PhD, Shigeto Shimmura, MD,† Jun Shimazaki, MD,† and Kazuo Tsubota, MD*‡*

Purpose: To study the modulation of immunoregulatory genes in ocular surface epithelial cells cultured on amniotic membrane (AM).

Methods: Microarray analysis was performed in a conjunctival epithelial cell line (CCL20.2) expanded on denuded AM. Among the genes that were upregulated by an AM substrate compared with collagen-coated dishes, the fetal nonclassic major histocompatibility complex molecule, HLA-G, was found to be the only immunoregulatory gene up-regulated by more than 2.5-fold. Because CCL20.2 is contaminated by HeLa cells, expression of HLA-G mRNA was confirmed in primary-cultured limbal (LE) and conjunctival epithelial (CE) cells by reverse transcriptase-polymerase chain reaction (RT-PCR), semiquantitative real-time PCR, immunocytochemistry, and Western blot analysis. A functional assay was performed using an HLA-G–transfected K-562 human erythroleukemia cell line.

Results: Freshly dissociated limbal epithelial cells express HLA-G mRNA; however, protein levels were low. Western blots and immunocytochemistry showed that both LE and CE cells upregulated the HLA-G protein when cultured on collagen-coated dishes and on AM. HLA-G mRNA levels were significantly higher in CE cultured on AM compared with collagen. Natural killer (NK) cell–induced cell lysis of an HLA class 1–negative K-562 human erythroleukemia cell line was slightly reduced when transfected with LE-derived HLA-G mRNA.

Conclusion: CE and LE cells express functional HLA-G when expanded ex vivo, which may affect inflammation and immune reaction when transplanted to the ocular surface.

Key Words: HLA-G, amniotic membrane, corneal epithelium, conjunctival epithelium, cornea immune responses

(*Cornea* 2006;25:715–721)

Numerous investigators have reported the use of amniotic membrane (AM) in ocular surface reconstruction since Kim and Tsengl[1] reinstated the technique in the modern era. AM is used mainly as either a graft, intended to function as a substrate for overlying epithelium, or as a patch to temporarily cover the ocular surface while the host tissue undergoes wound healing. The use of AM was integral in our experience with allograft limbal transplantation (ALT) for reconstructing the ocular surface in severe cicatricial disease.[2–4] AM is also used as a carrier for transplanting ex vivo cultured sheets of corneal epithelium[5] and oral mucosa epithelium.[6]

The effects of AM on the ocular surface were initially perceived as somewhat of a "black box," with many undefined characteristics of both soluble and nonsoluble components of AM cells and stroma. The anti-inflammatory actions of AM have been associated with the production of various cytokines,[7] regulation of growth factor expression,[8,9] and the release of proteinase inhibitors.[10] Direct interaction of AM with invading inflammatory cells may be involved in the elimination of leukocytes from the ocular surface.[11,12] Another important aspect of using AM on the ocular surface is its antiangiogenic property,[13–15] which is vital in maintaining a transparent ocular surface, and may work in suppressing immunologic rejection of allogenic cells and tissue.

To further explain the effects of AM, we hypothesized that AM may have direct immune-regulatory functions on surrounding cells when transplanted to the ocular surface. It is well documented that placental tissue, including AM, suppresses the semi-allo-immune response of the mother against the fetus.[16,17] Ueta et al[18] indicated that human AM is capable of inhibiting alloreactive T-cell response including cell division, proliferation, and T_H1/T_H2 cytokine synthesis in vitro. On the basis of these findings, we sought to study the expression and function of HLA-G, an immunoregulatory protein found to be upregulated in an initial screening by microarray analysis of cells cultured on AM.

MATERIALS AND METHODS

Cell Culture

The JAR (HLA-G$^-$) choriocarcinoma cell line, the JEG-3 (HLA-G$^+$) choriocarcinoma cell line, and the CCL20.2 conjunctival cell line were purchased from ATCC (American Type Culture Collection, Rockville, MD). Denuded AM was prepared as previously described.[19] Preserved AMs were rinsed in phosphate-buffered saline (PBS; 3 times), spread onto culture dishes, frozen at −80°C, and air-dried at room temperature. AM-coated dishes were stored at −80°C until use. Corneoscleral tissue from human donor eyes was obtained from Northwest Lions Eye Bank, and limbal rims were

Received for publication April 13, 2005; accepted November 23, 2005.
From the *Cornea Center, Tokyo Dental College, Chiba, Japan; the †Department of Ophthalmology, Tokyo Dental College, Chiba, Japan; and the ‡Department of Ophthalmology, Keio University School of Medicine, Tokyo, Japan.
Supported by a grant from the Japan Health Sciences Foundation and by a grant of the Ministry of Health and Walfare (Saisei, H15-13).
Reprints: Shigeto Shimmura, MD, Cornea Center, Ichikawa General Hospital, Tokyo Dental College, 5-11-13 Sugano, Ichikawa, Chiba 272-8513 Japan (e-mail: shimmura@tdc.ac.jp).

preserved for experiments after the central corneal button was used for corneal transplantation. After careful removal of excess sclera, iris, and corneal endothelium, limbal segments were placed in either collagen-coated dishes (Iwaki; Asahi Technoglass, Funabashi, Japan) or on AM-coated dishes. Limbal explants were cultured for 2 weeks at 37°C, 5% CO_2 in supplemented hormonal epithelial medium (SHEM), made of an equal volume of HEPES-buffered Dulbecco's modified Eagle's medium (DMEM) and Ham's F12 (Invitrogen, Carlsbad, CA) containing bicarbonate, 0.5% dimethylsulfoxide (Sigma, St. Louis, MO), 10 ng/mL human epidermal growth factor (EGF; Invitrogen), 5 μg/mL insulin (Sigma), 100 ng/mL cholera toxin (Invitrogen), 15% fetal bovine serum (FBS), 70 μg/mL penicillin (Wako Pure Chemical Industries, Osaka, Japan), and 140 ng/mL streptomycin (Wako). Expanded cells were cultured serum-free for 3 days in Epilife containing HCGS (Kurabo Co., Osaka, Japan) at 37°C, 5% CO_2.

Microarray Analysis

The Atlas Glass Total RNA Isolation Kit (BD, Franklin Lakes, NJ) was used to isolate total RNA from CCL20.2 cells cultivated on either collagen or AM-coated dishes. After RNA was isolated, genomic DNA was removed using DNAse (Qiagen, Hilden, Germany). The targets were prepared using the Atlas Glass Fluorescent Labeling Kit (Clontech Laboratories). Aminoallyl-dUTP was incorporated during first-strand cDNA synthesis. Fluorescent dye (Cy3 or Cy5) was covalently coupled to aminoallyl-dUTP in the first-strand cDNA. Absorbance of each target was determined by optical density measurements at 260 nm (DNA) and either 550 (Cy3) or 650 nm (Cy5). The total dye content (pmoles), amount of probe (nanograms), and specific activity (number of Cy molecules incorporated per number of bases) was calculated for each target synthesized. Once the target quality was determined to be appropriate, targets were hybridized to probes immobilized on glass slides. The slides were hybridized overnight at 50°C using the GlassHyb Hybridization Solution (BD). After we quantified gene expression with Atlas Glass Microarrays, analysis and visualization of data were done by the Atlas Navigator software (BD). The fluorescence intensity of each spot was calculated using the histogram quantitation method, which has the major advantage of being simple and stable.

Reverse Transcriptase-Polymerase Chain Reaction and Real-Time Polymerase Chain Reaction

Total RNA was isolated from cells using the SV total RNA isolation system (Promega, Madison, WI) according to the manufacturer's recommendations and verified by electrophoresis in denaturing 1.0% agarose gel. cDNA was prepared from total RNA with oligo(dT) priming and AVM reverse transcriptase (RT) XL (Takara, Bio, Ptsu, Shiga, Japan) by incubation of a 25-μL mixture at 41°C for 1 hour. The cDNA was subjected to polymerase chain reaction (PCR) by using the following HLA-G–specific oligonucleotide primers: forward primer 5′-cgcggaccaaccctcttcctgctactctcgg-3′ and reverse primer 5′-cggggtaccgcctcgctctggttggtagtagcc-3′. PCR amplifications (1 μL of cDNA in a total reaction volume of 50 μL) were run at 98°C for 10 seconds, at 56°C for 20 seconds, and at 72°C for 30 seconds (30 cycles). The amplification of β-actin was performed in the same manner to check cDNA quality. JAR cells were used as negative control, and JEG-3 cells were used as positive control. PCR amplification products were separated by electrophoresis on a 2% agarose gel.

Real-time RT-PCR was used to semiquantify HLA-G expression in primary cultured limbal and conjunctival epithelium. The method allows for the direct detection of PCR products during the exponential phase of the reaction, combining amplification and detection using TaqMan chemistry (Applied Biosystems, Foster City, CA) and the ABI Prism 7700 Sequence Detection System (Applied Biosystems). The TaqMan probe was designed to anneal to the target sequence, HLA-G α−1 domain, between the classic forward and reverse primers.

Immunocytochemistry

Cytospin preparations of limbal epithelial cells (5.0×10^4 cells/slide) were prepared by Auto Smear CF-12D (Sakura Finetechnical, Tokyo, Japan). Samples were fixed in cold acetone for 10 minutes and washed with PBS. Cytospin preparations were blocked with 10% normal donkey serum (Chemicon International, Temecula, CA) for 1 hour. Sections were incubated for 60 minutes at room temperature with a monoclonal antibody (MEM-G/9, 1/100 dilution; Abcam, Cambridge, UK) that reacts with the native form of human HLA-G on the cell surface, as well as with soluble HLA-G molecules. Isotype normal mouse immunglobulin G1 (IgG1) (Dako Cytomation, Glostrup, Denmark) was used as control. After washing with TBST (0.825 mmol/L Tris, 136.9 mmol/L NaCl, 1.34 mmol/L KCl, 0.1% Tween 20; Sigma), the section was reacted with rhodamine-conjugated donkey anti–mouse IgG secondary antibody (Jackson Immuno Research, West Grove, PA) for 30 minutes at room temperature. After 3 washes with TBST, the sections were incubated with 1 μg/mL 4′,6-diamidino-2-phenylindole (DAPI; Dojindo Laboratories, Tokyo, Japan) at room temperature for 5 minutes. Finally, sections were washed 3 times in TBST, and a coverslip was fixed using an antifading mounting medium (50 mmol/L Tris buffer saline, 90% glycerin [Wako], 10% 1,4-diazabicyclo (2,2,2) octane [Wako]).

Western Blot Analysis

Samples were dissolved with lysis buffer (50 mmol/L Tris-HCl, pH 7.4, 150 mmol/L NaCl, 1% Nonidet P-40; Calbiochem, Darmstadt, Germany) and homogenated. Samples were incubated for 40 minutes at 4°C and centrifuged at 15,000 rpm for 30 minutes at 4°C. Protein concentration of the supernatant was determined by the DC protein assay (Bio-Rad Laboratory, Hercules, CA). All samples were diluted in 2× sample buffer (100 mmol/L Tris-HCl [pH 6.8], 4% sodium dodecyl sulfate [Invitrogen], 20% glycerol [Wako], 12% 2-mercaptoethanol [Wako]) and boiled. Twenty micrograms of each sample was loaded on a Novex NuPAGE 10% Bis-Tris gel (Invitrogen) and transferred onto polyvinylidene difluoride (PVDF) membranes (Millipore, Billerica, MA). Membranes were blocked with 5% skim milk (Difco Laboratories, Detroit, MI), 1.5% normal goat serum, and PBS for 60 minutes at room

temperature. Membranes were reacted with an anti–HLA-G (MEM-G1) antibody (Serotec, Oxford, UK) for 60 minutes at room temperature. After 3 washes in TBST, donkey biotinylated anti–mouse IgG (Jackson ImmunoResearch) was added for 30 minutes at room temperature. Protein bands were visualized by the Vectastain ABC Elite Kit (Vector Laboratories, Bulingame, CA) and DAB (Vector Laboratories) as substrate.

Transfectants

The K-562 human erythroleukemia cell line (ATCC) was maintained in IMDM (Invitrogen) supplemented with 100 IU/mL penicillin (Wako)/100 μg/mL streptomycin (Wako) and FCS (Sanko Zyunyaku Co. Ltd., Tokyo, Japan). After successful amplification of the full-length human *HLA-G* gene from corneal epithelium, HLA-G plasmids were generated by cloning HLA-G cDNA into a green fluorescent protein (GFP) construct (phrGFP1-Puromycin; Stratagene, La Jolla, CA). GFP vector transfectants (phrGFP1-Puromycin) were used as control. Transfection was done using the Effectene Transfection Reagent (Qiagen) and the Nucleofector electroporation device (Amaxa, Cologne, Germany). Cells were selected in media containing 100 μg/mL Puromycin (Sigma).

Peripheral Blood Mononuclear Cells and Purified Natural Killer Cells

Peripheral blood mononuclear cells (PBMCs) were isolated from normal healthy volunteers by density gradient centrifugation using Ficoll-Paque PLUS (Amersham Biosciences, Uppsala, Sweden). $CD56^+$ natural killer (NK) cells were purified using the NK cell isolation kit II (Miltenyi Biotec, Bergisch Gladbach, Germany). Purity of the isolated populations used in the experiments was greater than 97% $CD3^-CD56^+$.

Cytotoxic Assay

The cytolytic action of NK cells against K-562 HLA-G transfectants was measured by bromodeoxyuridine (BrdU) release using the Cellular DNA Fragmentation enzyme-linked immunosorbent assay kit (Roche, Mannheim, Germany), in which effector cells (NK cells) were mixed with 1×10^5 BrdU-labeled target cells (K-562 transfectants) at the same effector:target ratio. After a 24-hour incubation at 37°C in a humidified 5% CO_2 incubator, DNA fragments by cell-mediated cytotoxicity were measured in the supernatant using a BrdU-specific monoclonal antibody. The percentage of cell lysis was calculated as follows: Percent specific lysis = [(OD_{450} experimental well − OD_{450} spontaneous release)/(OD_{450} maximum release − OD_{450} spontaneous release)] × 100.

RESULTS

Microarray Analysis

To screen for changes in gene expression by ocular surface epithelial cells under different culture conditions, CCL20.2 cells were cultured on either collagen- or AM-coated dishes and compared by microarray. Table 1 shows a list of genes that were upregulated by an AM substrate. There was a 2.6-fold increase in HLA-G expression, which was the only gene with a known immunoregulatory function. Because ATCC warns of a possible contamination of CCL20.2 cells by HeLa cells, we further studied the expression of HLA-G in freshly dissociated limbal epithelial cells, as well as primary cultures of limbal and conjunctival epithelial cells.

Cultured Conjunctival and Limbal Epithelial Cells Express HLA-G mRNA

HLA-G mRNA was expressed by primary conjunctival and limbal epithelial cells when cultured on collagen, as well as AM (Fig. 1). Freshly dissociated limbal epithelial cells also expressed HLA-G by RT-PCR. JAR cells (HLA-G negative) and K562 cells (HLA class I negative) were used as a negative control and JEG-3 cells were used as a positive control. No mRNA was detected from AM samples without seeded cells (data not shown), ruling out the possibility of contamination by AM mRNA.

Real-time PCR was used to semiquantitate HLA-G expression by each cell type when cultured on AM. In accordance with microarray results, CCL20.2 showed a 2.0-fold increase ($P < 0.05$) in HLA-G expression when cultured on AM (Fig. 2A). Similarly, primary conjunctival epithelial cells underwent a 1.9-fold increase ($P < 0.05$). Primary cultured limbal epithelial cells also had a tendency for upregulating HLA-G, but the difference was not statistically significant compared with collagen (Fig. 2A).

HLA-G Protein Expression by Limbal Epithelial Cells

Immunocytochemistry was done on cytospin samples of cultured primary limbal cells, JAR cells, and JEG-3 cells. Conjunctival cells were not available because of the scarcity of surgically removed tissue. Although freshly dissociated limbal cells did not express appreciable levels of HLA-G on the cell surface (Fig. 3A), primary limbal epithelial cells cultured on AM showed clusters of positive-staining cells (Fig. 3B). The specificity of HLA-G staining was confirmed by negative (JAR) and positive (JEG-3) controls (Fig. 3C and D). HLA-G protein was also compared by Western blot (Fig. 4). Similar to immunocytochemistry, HLA-G was detected in cultured limbal epithelial cells, but not by freshly dissociated cells from limbal tissue.

Inhibition of Cell Lysis by HLA-G–Transfected K-562 Cells

To show the immunosuppressive function of the HLA-G molecule, we transfected the *HLA-G* gene derived from limbal epithelium into the HLA class I–negative K-562 cell by using a GFP vector. HLA-G was successfully transfected into K-562 as shown by RT-PCR (Fig. 5A). When activated NK cells isolated from fresh peripheral blood were cocultured with transfected K-562, cell lysis detected by BrdU release was slightly lower in HLA-G–transfected cells than in control (Fig. 5B).

DISCUSSION

The absence of a harmful maternal immune response against the semiallogenic fetus has long been a major enigma in current biology. During mammalian pregnancy, fetal cells invade the uterine structures and survive without immunologic rejection.[20] It has now become evident that trophoblast cells

TABLE 1. Alteration of Genes in Microarray Analysis

GenBank #	Gene	Ratio (AM/dish)
NM_005876	Nuclear protein, marker for differentiated aortic smooth muscle and downregulated with vascular injury	2.5
NM_001174	Rho GIPase activating protein 6	2.9
NM_000156	Guadinoacetate *N*-methyltransferase	2.6
NM_000407	Glycoprotein 1b [platelet], β-polypeptide	3.8
NM_000733	CD3E antigen, epsilon polypeptide [TiT3 complex]	3.0
NM_000741	Cholinergic receptor, muscarinic 4	3.5
NM_004357	CD 151 antigen	2.7
NM_003822	Nuclear receptor subfamily 5, group A, member 2	2.7
NM_004456	Enhancer of zeste (*Drosophila*) homolog 2	3.3
NM_001731	B-cell translocation gene 1, antiproliferative	3.9
NM_001615	Actin, gamma 2, smooth muscle, enteric	3.2
NM_001567	Inositol polyphosphate phosphatase-like 1	0.4
NM_002282	Keratin, hair, basic, 3	2.8
NM_005576	Lysyl oxidase-like 1	0.2
NM_002127	HLA-G histocompatibility antigen, class I, G	2.6
NM_000290	Phosphoglycerate mulase 2 [muscle]	2.9
NM_002499	Neogenin (chicken) homolog 1	3.0
NM_002571	Progestagen-associated endometrial protein (placental protein 14, pregnancy-associated endometrial α-2-globulin, α uterine protein)	3.5
NM_002722	Pancreatic polypeptide	4.9
NM_002824	Parathymosin	2.7
NM_002846	Protein tyrosine phophatase, receptor type, N	2.8
NM_005394	Postmeiotic segregation increased 2-like 8	2.5
NM_001051	Somatostatin receptor 3	4.7
NM_002911	Regulator of nonsense transcripts 1	4.0
NM_003006	Selectin P ligand	4.9
NM_003178	Synapsin II	2.5
NM_003281	Troponin I, skeletal, slow	3.6
NM_006945	Small proline-rich protein 2B	3.4
NM_003611	Chromosome X open reading frame 5	3.7

express the nonclassical class 1 HLA molecules HLA-G[21,22] and HLA-E[23] and the classic class 1 HLA molecule HLA-C, which is expressed mainly during the first trimester.[24,25] The role of HLA-G in the fetal membrane is to protect cytotrophoblasts against NK cytolysis by maternal NK cells.[26] Indeed, the expression of HLA-G on the cell surface of various cells protected susceptible target cells from NK-mediated cytotoxicity.[27–31]

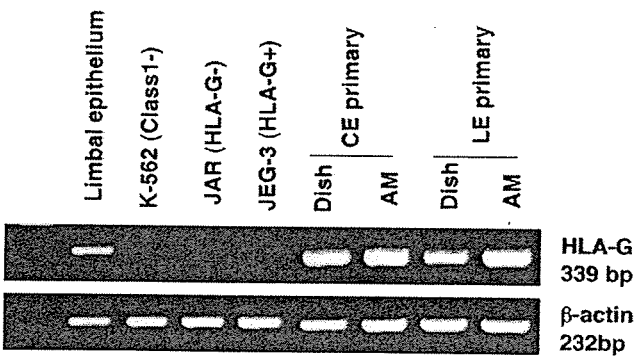

FIGURE 1. RT-PCR of HLA-G mRNA from primary LE and CE cultures (P0) on collagen and AM. JAR and K562 cells (HLA class 1 negative) were loaded as negative control and JEG-3 was loaded as positive control. Freshly dissociated limbal epithelium also expressed HLA-G mRNA.

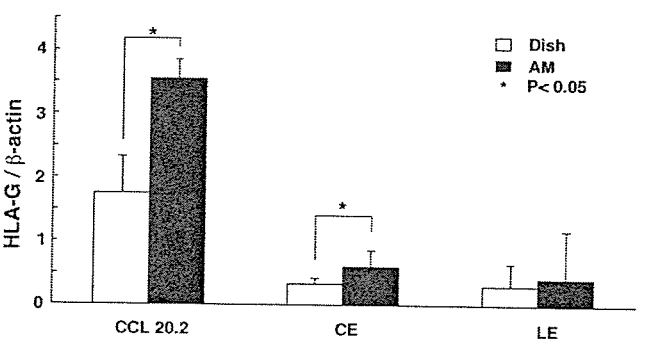

FIGURE 2. Semiquantitative real-time RT-PCR of HLA-G in CCL20.2, primary LE, and CE cells. HLA-G expression increased significantly in CCL20.2 and CE when cultured on AM instead of collagen. Although a similar trend was observed in LE, the increase was not statistically significant. Mean ± SD (n = 5). *$P < 0.05$.

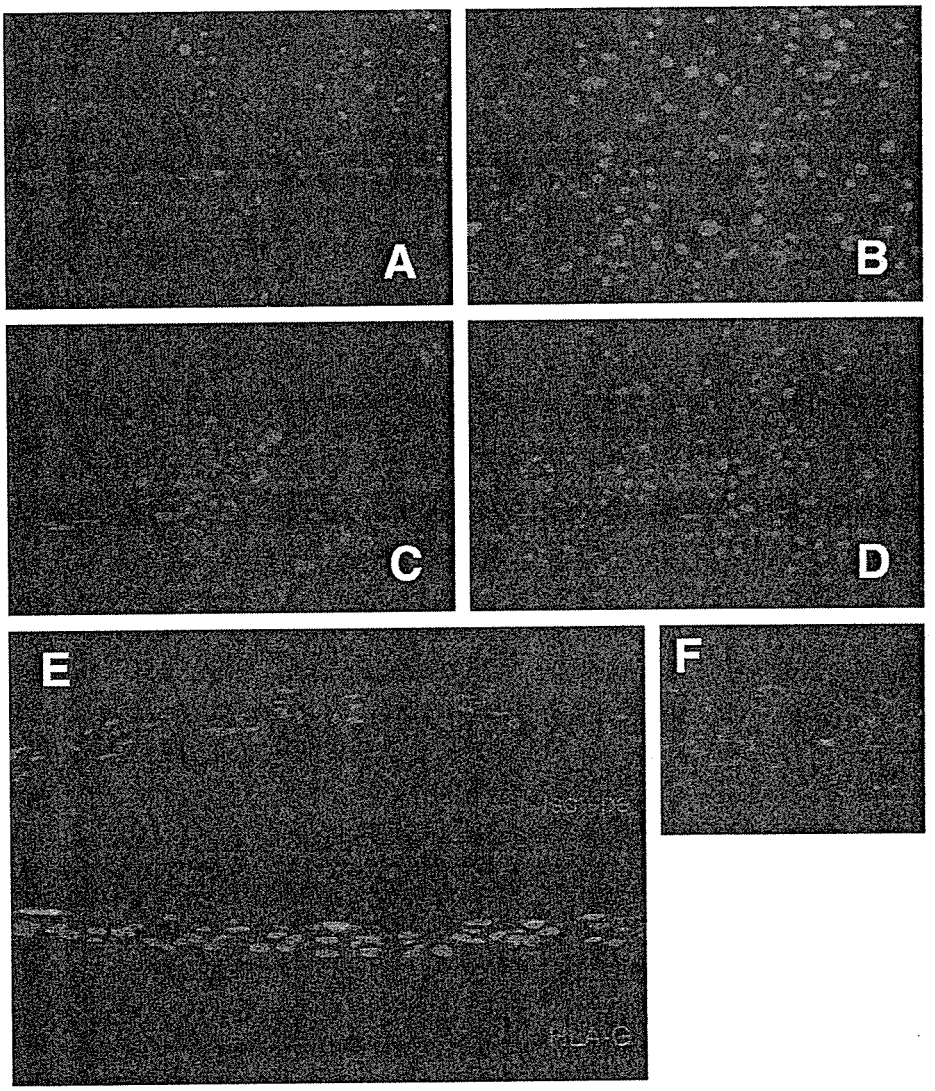

FIGURE 3. Immunocytochemistry of HLA-G in cytospin samples of freshly dissociated limbal epithelium (A) and primary cultures (P0) of LE cells explanted on AM (B). JAR, HLA-G–negative control (C); JEG-3, HLA-G–positive control (D). E, Immunocytochemistry in primary cultured limbal epithelial cells. (F), Positive control using placental tissue. Original magnification, ×200.

HLA-G can be expressed by adult tissue in the presence of inflammation or when cells are cultivated in vitro where the expression of HLA-G is selectively upregulated by cytokines such as interferon-γ[32] and interleukin-10.[33] One such example was reported by Wiendl et al,[34] who recently showed that muscle fibers in inflammatory myopathies and cultured myoblasts express the HLA-G molecule. In this report, we showed the upregulation of HLA-G in cultivated conjunctival and corneal cells. It is interesting that only HLA-G mRNA was upregulated when an AM substrate was used, whereas other class 1 HLA molecules, namely HLA-C and HLA-E, slightly decreased on microarray analysis (data not shown). We used the CCL20.2 conjunctival cell line for microarrays because a large number of cells was required as a source of RNA, which was not possible with primary cultured cells. Because CCL20.2 cells are contaminated by HeLa cells, we confirmed the expression of HLA-G mRNA in primary cultured conjunctival and limbal cells by RT-PCR and Western blots. Conjunctival cells expressed significantly higher levels of HLA-G on AM- than on collagen-coated dishes when measured by real-time PCR. The same trend was observed in limbal cells; however, the difference was not statistically significant. The upregulation of HLA-G was not a contamination by native AM RNA, because the AM used in the study was extensively processed to remove cellular components, and RT-PCR of AM samples alone did not yield any RNA bands.

According to another report, immunohistochemical analysis carried out on corneas showed positive immunohistochemical staining with anti–HLA-G antibodies.[35] However, we were not able to detect HLA-G in cornea tissue sections (data not shown) or cytospin samples of epithelial cells by immunohistochemistry. Western blot analysis detected the HLA-G protein only in cultured cells as well. HLA-G was also detected in primary cultured limbal epithelial cells (Fig. 3). This discrepancy may be caused by different epitopes recognized by the antibodies used. However, because HLA-G

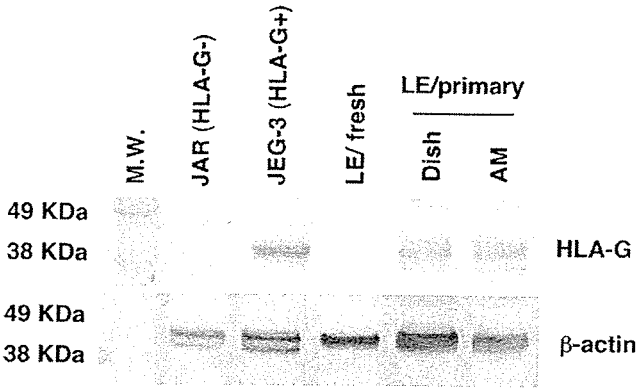

FIGURE 4. Western blot of HLA-G protein in limbal epithelium and primary cultured LE cells expanded on plastic and AM. Samples were loaded with 20 mg of protein/lane. HLA-G protein was detected in cultured LE, but not in freshly dissociated limbal epithelium. β-actin was run as internal control. JAR, HLA-G–negative control; JEG-3, HLA-G–positive control.

mRNA was detected in freshly dissociated cells by RT-PCR, it is possible that the cornea may express HLA-G in vivo under inflammatory conditions. The staining pattern of HLA-G in cytospin samples and primary cultures (Fig. 3) was not strictly localized to the cell membrane as shown in the placenta-positive control. This result may have been caused by incomplete trafficking of HLA-G to the cell membrane in corneal epithelial cells.

We showed that gene transfer of cornea-derived HLA-G into K-562 cells slightly inhibited lysis by NK cells in vitro. This effect was also shown in another study,[26] as well as in HLA-G transfected primary human myoblasts.[34] This model was used because K-562 cells are void of membrane-bound HLA molecules, allowing for the analysis of HLA-G alone, without the involvement of other HLA molecules. The results suggest that HLA-G expressed on cultivated sheets may block the lytic activity of NK cells after transplantation to the ocular surface. There are reports that suggest the involvement of NK cells in allograft rejection after keratoplasty in rodents.[36,37] Clinically, soluble HLA-G levels in serum and biopsy samples were shown to correlate with graft survival in cardiac transplant patients.[38] Although our results did not reach statistical significance, this may have been caused by inadequate protein upregulation by transfection. However, the objective of this experiment was to show partial functional upregulation by transfection of the *HLA-G* gene obtained directly from corneal epithelial cells.

Cultivated sheet transplantation has become another tool in the treatment of ocular surface disease. AM is often used as a carrier; however, other substrates such as fibrin[39] and temperature-sensitive polymers[40] have been reported. It is possible that the upregulation of HLA-G is not a specific response to AM carriers; however, a statistically greater enhancement was observed in conjunctival cells in our study. Although further studies are required to elucidate the precise mechanisms involved, HLA-G upregulation may be an advantage of ex vivo cultivated sheets over direct transplantation of epithelial tissue.

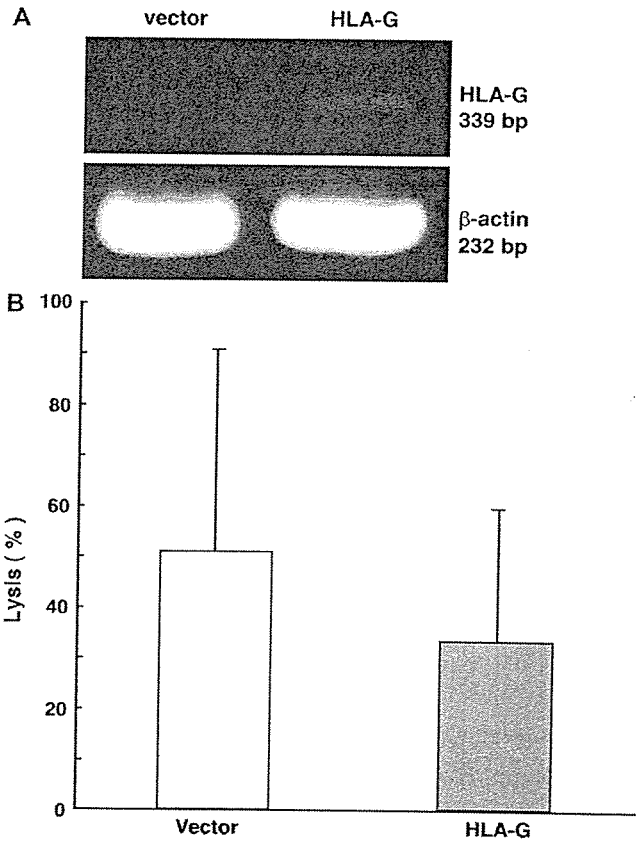

FIGURE 5. Class 1–negative K562 cells were transfected with an HLA-G construction vector or a vector-only negative control. (A), RT-PCR of HLA-G in transfectants. (B), Cytolysis of K562 cells by CD56-+ NK cells was inhibited by HLA-G expression. Data are expressed as mean ± SD (n = 4).

ACKNOWLEDGMENTS

The authors thank Mifuyu Oshima and Hiroe Fujikawa for technical assistance and the staff of the Cornea Center Eye Bank for administrative support.

REFERENCES

1. Kim JC, Tseng SC. Transplantation of preserved human amniotic membrane for surface reconstruction in severely damaged rabbit corneas. *Cornea*. 1995;14:473–484.
2. Tsubota K, Satake Y, Ohyama M, et al. Surgical reconstruction of the ocular surface in advanced ocular cicatricial pemphigoid and Stevens-Johnson syndrome. *Am J Ophthalmol*. 1996;122:38–52.
3. Shimazaki J, Yang HY, Tsubota K. Amniotic membrane transplantation for ocular surface reconstruction in patients with chemical and thermal burns. *Ophthalmology*. 1997;104:2068–2076.
4. Tseng SC, Prabhasawat P, Barton K, et al. Amniotic membrane transplantation with or without limbal allografts for corneal surface reconstruction in patients with limbal stem cell deficiency. *Arch Ophthalmol*. 1998;116:431–441.
5. Koizumi N, Inatomi T, Quantock AJ, et al. Amniotic membrane as a substrate for cultivating limbal corneal epithelial cells for autologous transplantation in rabbits. *Cornea*. 2000;19:65–71.
6. Nakamura T, Endo K, Cooper LJ, et al. The successful culture and autologous transplantation of rabbit oral mucosal epithelial cells on amniotic membrane. *Invest Ophthalmol Vis Sci*. 2003;44:106–116.

7. Fortunato SJ, Menon R, Lombardi SJ. Interleukin-10 and transforming growth factor-beta inhibit amniochorion tumor necrosis factor-alpha production by contrasting mechanisms of action: therapeutic implications in prematurity. *Am J Obstet Gynecol*. 1997;177:803–809.
8. Yam HF, Pang CP, Fan DS, et al. Growth factor changes in ex vivo expansion of human limbal epithelial cells on human amniotic membrane. *Cornea*. 2002;21:101–105.
9. Tseng SC, Li DQ, Ma X. Suppression of transforming growth factor-beta isoforms, TGF-beta receptor type II, and myofibroblast differentiation in cultured human corneal and limbal fibroblasts by amniotic membrane matrix. *J Cell Physiol*. 1999;179:325–335.
10. Kim JS, Kim JC, Na BK, et al. Amniotic membrane patching promotes healing and inhibits proteinase activity on wound healing following acute corneal alkali burn. *Exp Eye Res*. 2000;70:329–337.
11. Shimmura S, Shimazaki J, Ohashi Y, et al. Antiinflammatory effects of amniotic membrane transplantation in ocular surface disorders. *Cornea*. 2001;20:408–413.
12. Higa K, Shimmura S, Shimazaki J, et al. Hyaluronic acid-CD 44 interaction mediates the adhesion of lymphocytes by amniotic membrane stroma. *Cornea*. 2005;24:206–212.
13. Ma DH, Yao JY, Yeh LK, et al. In vitro antiangiogenic activity in ex vivo expanded human limbocorneal epithelial cells cultivated on human amniotic membrane. *Invest Ophthalmol Vis Sci*. 2004;45:2586–2595.
14. Shao C, Sima J, Zhang SX, et al. Suppression of corneal neovascularization by PEDF release from human amniotic membranes. *Invest Ophthalmol Vis Sci*. 2004;45:1758–1762.
15. Kobayashi N, Kabuyama Y, Sasaki S, et al. Suppression of corneal neovascularization by culture supernatant of human amniotic cells. *Cornea*. 2002;21:62–67.
16. Sionov RV, Yagel S, Har-Nir R, et al. Trophoblasts protect the inner cell mass from macrophage destruction. *Biol Reprod*. 1993;49:588–595.
17. Beer AE, Sio JO. Placenta as an immunological barrier. *Biol Reprod*. 1982;26:15–27.
18. Ueta M, Kweon MN, Sano Y, et al. Immunosuppressive properties of human amniotic membrane for mixed lymphocyte reaction. *Clin Exp Immunol*. 2002;129:464–470.
19. Shimazaki J, Aiba M, Goto E, et al. Transplantation of human limbal epithelium cultivated on amniotic membrane for the treatment of severe ocular surface disorders. *Ophthalmology*. 2002;109:1285–1290.
20. Bainbridge DR. Evolution of mammalian pregnancy in the presence of the maternal immune system. *Rev Reprod*. 2000;5:67–74.
21. Chumbley G, King A, Holmes N, et al. In situ hybridization and northern blot demonstration of HLA-G mRNA in human trophoblast populations by locus-specific oligonucleotide. *Hum Immunol*. 1993;37:17–22.
22. Ellis SA, Palmer MS, McMichael AJ. Human trophoblast and the choriocarcinoma cell line BeWo express a truncated HLA Class I molecule. *J Immunol*. 1990;144:731–735.
23. King A, Allan DS, Bowen M, et al. HLA-E is expressed on trophoblast and interacts with CD94/NKG2 receptors on decidual NK cells. *Eur J Immunol*. 2000;30:1623–1631.
24. King A, Burrows TD, Hiby SE, et al. Surface expression of HLA-C antigen by human extravillous trophoblast. *Placenta*. 2000;21:376–387.
25. King A, Boocock C, Sharkey AM, et al. Evidence for the expression of HLAA-C class I mRNA and protein by human first trimester trophoblast. *J Immunol*. 1996;156:2068–2076.
26. Rouas-Freiss N, Goncalves RM, Menier C, et al. Direct evidence to support the role of HLA-G in protecting the fetus from maternal uterine natural killer cytolysis. *Proc Natl Acad Sci USA*. 1997;94:11520–11525.
27. Pazmany L, Mandelboim O, Vales-Gomez M, et al. Protection from natural killer cell-mediated lysis by HLA-G expression on target cells. *Science*. 1996;274:792–795.
28. Munz C, Holmes N, King A, et al. Human histocompatibility leukocyte antigen (HLA)-G molecules inhibit NKAT3 expressing natural killer cells. *J Exp Med*. 1997;185:385–391.
29. Perez-Villar JJ, Melero I, Navarro F, et al. The CD94/NKG2-A inhibitory receptor complex is involved in natural killer cell-mediated recognition of cells expressing HLA-G1. *J Immunol*. 1997;158:5736–5743.
30. Pende D, Siveri S, Accame L, et al. HLA-G recognition by human natural killer cells. Involvement of CD94 both as inhibitory and as activating receptor complex. *Eur J Immunol*. 1997;27:1875–1880.
31. Soderstrom K, Corliss B, Lanier LL, et al. CD94/NKG2 is the predominant inhibitory receptor involved in recognition of HLA-G by decidual and peripheral blood NK cells. *J Immunol*. 1997;159:1072–1075.
32. Yang Y, Chu W, Geraghty DE, et al. Expression of HLA-G in human mononuclear phagocytes and selective induction by IFN-gamma. *J Immunol*. 1996;156:4224–4231.
33. Moreau P, Adrian-Cabestre F, Menier C, et al. IL-10 selectively induces HLA-G expression in human trophoblasts and monocytes. *Int Immunol*. 1999;11:803–811.
34. Wiendl H, Mitsdoerffer M, Hofmeister V, et al. The non-classical MHC molecule HLA-G protects human muscle cells from immune-mediated lysis: implications for myoblast transplantation and gene therapy. *Brain*. 2003;126:176–185.
35. Le Discorde M, Moreau P, Sabatier P, et al. Expression of HLA-G in human cornea, an immune-privileged tissue. *Hum Immunol*. 2003;64:1039–1044.
36. Larkin DF, Calder VL, Lightman SL. Identification and characterization of cells infiltrating the graft and aqueous humour in rat corneal allograft rejection. *Clin Exp Immunol*. 1997;107:381–391.
37. Claerhout I, Kestelyn P, Debacker V, et al. Role of natural killer cells in the rejection process of corneal allografts in rats. *Transplantation*. 2004;77:676–682.
38. Lila N, Carpentier A, Amrein C, et al. Implication of HLA-G molecule in heart-graft acceptance. *Lancet*. 2000;355:2138.
39. Rama P, Bonini S, Lambiase A, et al. Autologous fibrin-cultured limbal stem cells permanently restore the corneal surface of patients with total limbal stem cell deficiency. *Transplantation*. 2001;72:1478–1485.
40. Nishida K, Yamato M, Hayashida Y, et al. Functional bioengineered corneal epithelial sheet grafts from corneal stem cells expanded ex vivo on a temperature-responsive cell culture surface. *Transplantation*. 2004;77:379–385.